UNIVERSITY OF SIENA
DEPARTMENT OF BIOTECHNOLOGY, CHEMISTRY AND PHARMACY

DOTTORATO DI RICERCA IN SCIENZE CHIMICHE E FARMACEUTICHE
XXXIII CICLO

DOCTORATE IN CHEMICAL AND PHARMACEUTICAL SCIENCES
XXXIII CYCLE

COORDINATOR: Prof. Maurizio Taddei

Use and characterisation of free or immobilised enzymatic systems for the synthesis and functionalisation of novel materials

SSD: CHIM/02

TUTOR:
Prof. Rebecca Pogni

CANDIDATE:
Jessica Costa

ACADEMIC YEAR: 2020/2021

INDEX

ACKNOWLEDGMENTS

This thesis presents the work I have been carrying during my Ph.D. program in the Department of Biotechnology, Chemistry and Pharmacy, University of Siena (Italy), under the supervision of Prof. Rebecca Pogni, and in the time spent as a visiting Ph.D. student in the Department of Bioproducts and Biosystems, Aalto University School of Chemical Technology (Finland), under the supervision of Prof. Monika Österbeg. A part of this research was performed under the FISH4FISH project, funded by the EU EMMFF-Blue Economy 2018 program.

There are many people whom I would like to thank for their contributions, both directly and indirectly, to this thesis. I would first like to thank my supervisor, Professor Rebecca Pogni, for the opportunity to conduct my Ph.D. study in her research group and for the support and guidance I have received over the years. I am thankful that I had the possibility of learning from her expertise and experience.

I would like to thank Professor Monika Österbeg and her research groups, with particular reference to Dr. Juan José Valle Delgado and Dr. Maria Morits, who guided me throughout my time in Finland, teaching me many new and important things.

I want also to thank Prof. Atrei for his contribution to the part of magnetic nanoparticles.

The next major thanks go to my scientific collaborators, Dr. Camilla Baratto and Maher Al Khatib.

A special thank goes also to my family and friends who had a fundamental role in getting me through the Ph.D. process successfully.

Jessica Costa

SUMMARY

The work reported in this Ph.D. thesis is focused on the use and immobilisation of enzymes to produce new materials, which are important for biotechnological applications.
The use of enzymes in industrial sectors is continuously increasing. Enzymes offer many advantages over traditional chemical processes. They are eco-compatible, show high product selectivity and the ability to operate in milder reaction conditions.
Two enzymes, belonging to the class of Oxidoreductases (EC1) and Hydrolases (EC3), Laccase and Chitinase of fungal origin respectively, have been studied in this Ph.D. thesis for their importance in biotechnological applications.
Laccase (EC 1.10.3.2) has several applications: delignification of lignocellulosic material, textile dye transformation, food technologic uses, waste detoxification, biosensor and medical care applications.
Chitinase (EC 3.2.1.14) catalyses the degradation of β-1→4 linkages in chitin and Chitosan with the formation of low Molecular Weight compounds named chitooligosaccharides (COS). The latter show improved antioxidant and antimicrobial activity.

The research work of this thesis can be divided into two parts. A schematic representation is reported at the end of this summary.

The first part is focused on the immobilisation of laccase and chitinase. The main object of enzymatic immobilisation is to enhance the economics of biocatalytic processes. Enzymatic immobilisation allows the reuse of enzymes for an extended period of time and enables easier separation of the catalyst from the product. Furthermore, immobilisation improves many properties of enzymes: performance in the organic solvents, pH tolerance and heat stability. The most widely used immobilisation method is the covalent binding of the enzyme to support. Different type of support can be chosen for enzymatic immobilisation. As

the material can plays a crucial role in the immobilisation process and the properties of the produced catalytic system.
In this thesis we have chosen two different supports: super paramagnetic nanoparticles for both the enzymes used and the chitosan beads as an alternative support for chitinase.
Magnetic nanoparticles show interesting properties for enzymatic immobilisation, they can be obtained with small size, increasing the yield of enzymatic immobilisation and above all, the reaction products can be easily recovered applying an external magnetic field.
Magnetic nanoparticles were prepared following the traditional method of co-precipitation of Fe^{2+} and Fe^{3+} ions. In addition, the MNPs surface was coated with (3-aminopropyl) triethoxysilane (APTES), so the amino groups on their surface allow the attack of linker such as glutaraldehyde, to facilitate the enzymatic binding. This immobilisation process was successfully used for chitinase, obtaining a high immobilisation yield and increasing enzymatic stability. Different was for laccase, which having a different catalytic mechanism a revision of the synthesis has been attempt. The use of the magnetic nanoparticles obtained with the traditional method hampered the detection of stable radical species formed during the catalytic mechanism as it happens for the oxidation product of 2,2'-azino-bis (3-ethylbenzothiazolin-6-sulfonic acid) (ABTS), the standard compound used to test the enzyme activity. Changing some synthetic parameters, the new magnetic nanoparticles were produced and characterised. In fact nanoparticles with a lower aggregation state and a smaller hydrodynamic diameter were obtained and tested without any interference with the ABTS substrate.
Chitinase was also immobilised on chitosan beads/Macro-Spheres (CMS), as this support is completely atoxic and so most suitable for application in food industries.
The presence of active amino groups in deacetylated GlcNAc units of chitosan also enables the binding of the linker (glutaraldehyde and genipin) and then of the enzyme. The goal of this part of the thesis was to attempt the immobilisation of Chitinase on different supports, MNPs and CMS, for the efficient production of COS.

The second part of this thesis is focused on the use of enzymes to produce melanin pigments. Melanins have a variety of biological functions, including protection against UV radiation, free radical scavengers and metal ions chelators. Thanks to their properties, melanins found applications in several fields such as cosmetics, optoelectronics, food, and pharmacology.
Eumelanin and Pheomelanin have been produced by oxidative enzymatic synthesis using laccase from *Trametes versicolor* and then characterised by the use of Multifrequency Continuos Wave (CW) and pulse Q-band EPR. Then, as soluble melanin pigments have important technological applications in different fields, like in optoelectonics, soluble pigments mimicking pyomelanin structure have been synthesized starting from Homogentisic Acid and Gentisic Acid monomers and spectroscopically characterised with their antioxidant activities determination.

At the end, the scientific productions and the list of articles published during this Ph.D. program are reported.

Scheme - Overview of the thesis work

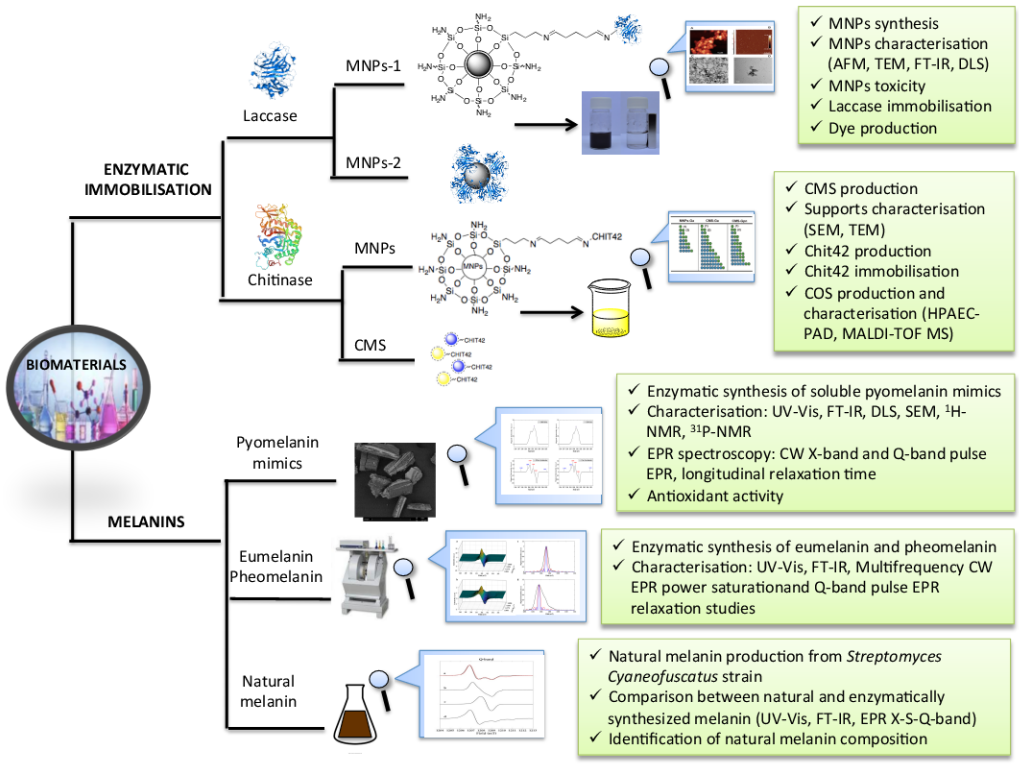

1.1 Enzymes

Based on the principles of green chemistry and suitable development, the use of enzymes represents a spectacular advance in industrial biotechnology [1]. Enzymes are biological macromolecules that catalyse chemical reactions. They found many industrial applications due to their important advantages compared to the chemical processes. They are derived from renewable resources, are biodegradable, work under relatively mild conditions of temperature and pH, and tend to offer high selectivity for their substrates [2,3].
According to the type of reactions that the enzymes catalyse, they are classified into seven categories reported in Table 1 [4,5].

Table 1 Enzymes Classification

	Types	Biochemical properties
EC1	Oxidoreductases	Catalyse redox reaction
EC2	Transferases	Transfer or exchange groups among some substrates
EC3	Hydrolases	Catalyse the hydrolysis of the substrate
EC4	Lyases	Promote the removal of the group from the substrate to leave a double bond reaction or catalyse its reverse reaction
EC4	Isomerases	Catalyse the formation of an isomer of a compound.
EC6	Ligases	Catalyse the association of two molecules
EC7	Translocase	Catalyse the movement of ions or molecules across membranes or their separation within membranes

This thesis is focused on the use of two enzymes, laccase and chitinase, belonging to the class of oxidoreductases and hydrolases respectively. They are involved in many important biotechnological applications such as lignin degradation and bioethanol production [6,7].

1.2 Laccase

Laccases (benzenediol: oxygen oxidoreductase. EC 1.10.3.2) are multicopper- containing oxidoreductases found in higher plants, bacteria, fungi, insects and lichens.
They find application in several industrial sectors such as food, pulp and paper, textile and cosmetics [8]. The potential applications of laccases in numerous and different biocatalytic processes for industry and environmental solutions has increased the interest in understanding their structure and mechanism of action. Laccase typically comprises four copper ions in their catalytic site. These coppers are classified as type 1 (T1), type 2 (T2) and binuclear type 3 (T3), according to their spectroscopic behaviour and role in catalysis. The initial electron acceptor in laccase-catalyzed oxidation is copper T1 located in the cavity close to the enzyme surface. The reduction of copper T1 is a rate-limiting step in the reactions catalysed by laccase [9]. In general, laccases oxidize a wide range of substrates, typically substituted phenols and aromatic amines, which are transformed into free radicals. Unstable chemical products and primarily generated free radicals commonly start other reactions, leading to complex chemical transformations of biological relevance such as lignin synthesis and degradation [10,11].
The overall laccase reaction involves one electron, sequential oxidations of four molecules of reducing substrates, concurrently with two double electron reductions of oxygen atoms into their respective H_2O molecules (Figure 1). This process is accompanied by a catalytic exchange of 4 H^+ equivalents [12]. It was also observed that substrates of laccase, such as 2,2'-azino-bis (3-ethylbenzothiazolin-6-sulfonic) (ABTS), radical 2,2,6,6-tetramethylpiperidine 1-oxyl (TEMPO) or violuric acid (VA) can act as mediators speeding up the catalytic reaction on several substrates and making possible the oxidation of compounds that otherwise would not be the substrate of this enzyme. Furthermore, the cationic ABTS radical, formed by laccase, has been completely characterised by EPR spectroscopy and the analysis confirmed that $ABTS^{+\cdot}$ is the more stable radical [13,14].

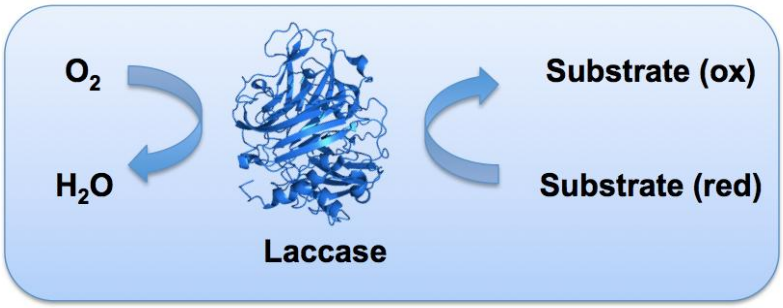

Figure 1 Catalytic mechanism of Laccase

Laccase was chosen with TEMPO as mediator for chemo-enzymatic oxidation of benzylamines to obtain imines and aldehydes and for the oxidation of primary and secondary alcohols to the corresponding carboxylic acids, ketones or aldehydes [15,16].
The importance of mediator was highlighted for the degradation of synthetic dyes in the waste-water application of laccase, where the oxidized species of mediator have a dominant role in the oxidation of non-phenolic aromatic compounds [17]. Laccase is not used only for decolouration dyes but also for their production. In fact, it catalyses not only catabolic processes such as depolymerisation and degradation but can also carry out various dimerization, oligomerization and polymerization reactions of some hundred aromatic substrates that synthesize new molecules with valuable functions [18], such as water soluble phenoxazine dyes and novel bioactive textile dyes with antioxidant and antimicrobial properties [19,20].
The efficiency of laccase oxidation generally depends on the type of substrate group, the position of the substitution and on its redox potential. Depending on the redox potential, laccases are divided into two groups: low and high redox potential enzymes. Low redox potential enzymes occur in bacteria, plants and insects, whereas high redox potential laccase is widely distributed in fungi [9].

1.3 Chitinase

Chitinases (EC 3.2.1.14) belongs to the class of glycosyl hydrolases (GH) because they are able to hydrolyse the glycosidic linkages in carbohydrates. Chitinases are widely present in nature. They have been

found in bacteria, viruses, fungi and plants and they participate in physiological processes such as nutrition, parasitism, morphogenesis and immunity [21–23].

They are specific for the β(1→4) glycosidic bonds present in chitin [24].

Chitin represents the second most abundant polysaccharide in nature after cellulose, as it is one of the main components of the exoskeleton of insects and crustaceans and it is also presents in some fungi. It is formed by N-acetyl-β-D-glucosamine (GlcNac) units linked by type β(1→4) glycosidic bonds [25–27].

Chitin has strong inter- and intra-molecular hydrogen bonding, which provides its insoluble property in inorganic and organic solvents. For that its deacetylated form, chitosan, is more widely used for industrial applications (Figure 2) [28]. Chitosan is a linear polysaccharide that contains copolymers of D-glucosamine (deacetylated units) and N-acetyl-D-glucosamine (acetylated units) linked by β (1→4) glycosidic bonds [29]. The deacetylation of chitosan is generally defined as the glucosamine/N-acetyl glucosamine ratio, which goes up as chitin is converted to chitosan. Therefore, when the percentage of N-acetyl glucosamine is higher than glucosamine, the biopolymer is called chitin and when the percentage of glucosamine exceeds N-acetyl glucosamine the compound is called chitosan [30].

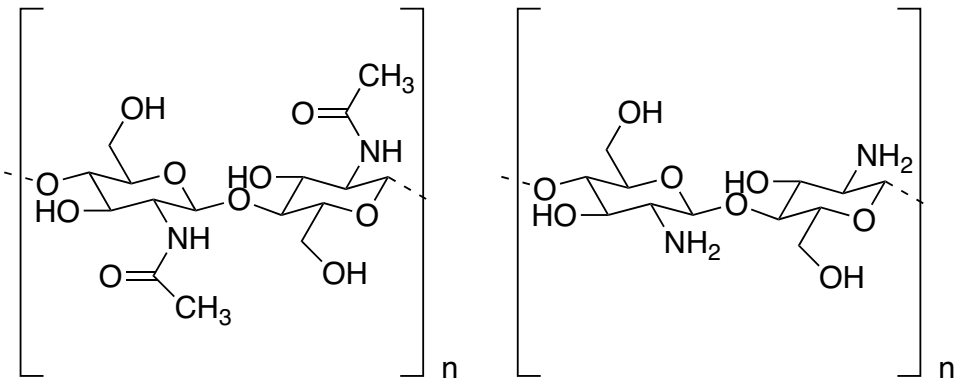

Chitin **Chitosan**

Figure 2 Chitin and chitosan structures

Thanks to their properties such as biocompatibility, non-toxicity, biodegradability and biological activities such as antimicrobials and antioxidants, these biopolymers can be considered as a new source of

functional materials. In fact, they are used in many sectors like pharmaceuticals, biomedical, cosmetic, food, textiles, agriculture, paper and enzymatic immobilisation [31].

Chitinases are responsible for the biotransformation of chitin or chitosan into chitooligosaccharides. According to their catalytic action, chitinases have been divided into two groups:

i. *Endo*-chitinases: cleave chitin at internal sites;
ii. *Exo*-chitinases: slit chitin from its reducing or non-reducing end.

The hydrolysis of chitin yields a series of chitooligosaccharides (COS) containing random GlcNAc and D-glucosamine (GlcN) units. Three families of COS can be differentiated: fully acetylated chitooligosaccharides (*fa*COS) formed exclusively by GlcNAc, partially acetylated chitooligosaccharides (*pa*COS) composed of GlcN and GlcNAc and fully deacetylated chitooligosaccharides (*fd*COS) formed exclusively by GlcN. The bioactivity of COS is well reported, in particular their anti-inflammatory, neuroprotective, antibacterial, antiviral, antihypertensive and antitumor properties. The size of COS defined by the degree of polymerization (DP), degree of deacetylation (DD) and pattern of acetylation (PA) exert a notable influence on their properties [32,33].
This thesis is focused on the use of a specific exo-chitinase Chit42 from fungus *Trichoderma harzianum* cloned in *Pichia* pastoris (in collaboration with the group at UAM (Spain)). This enzyme hydrolysed chitin and chitosan with a low DD giving rise to mixtures enriched in *fa*COS and *pa*COS, respectively [34].

Chitinases have shown immense potential for a wide range of applications involving food and medicine. Applications using chitinase-based processing are economic, eco-friendly, and non-hazardous.
Chitinases can be used for a number of human healthcare applications such as the production of ophthalmic preparations with microbicides. Thanks to its antifungal activity, chitinase can be combined with

antifungal drugs and used as a therapeutic treatment for various fungal infections [35,36].
Chitinases are also attaining prominence in the field of biotechnology applied in waste management and pest control in agriculture [22].

1.4 Enzymatic immobilisation

As reported in the previous paragraphs, enzymes find useful applications in different fields. However, two critical parameters that limit their application are quantity and quality. For industrial-scale processes, enzymes in tons and their extreme purity are required. This leads to an increase in the cost of the process. One of the solutions made to solve these problems was enzymatic immobilisation [37].

In the last two decades, the immobilisation of enzymes is an important challenge in biotechnology. The aim of this technique is to obtain reusable and stable enzymes with resistance to different reaction environment. Immobilisation improves many properties of enzymes such as pH tolerance, heat stability, functional stability and performance in organic solvents, furthermore stabilizing the structural rigidity of enzyme prevents his dissociation and inactivation [38,39].
The methods of enzyme immobilisation can be divided into three categories:

i. Binding to a support
ii. Entrapment
iii. Cross-linking

Binding to support can be physical, ionic and covalent. Generally, the stronger is the covalent binding because physical and ionic are too wear to keep the enzyme fixed under extreme industrial conditions. However, covalent binding has a disadvantage, linking the enzyme with support can change the active conformation losing its activity.
Entrapment *via* inclusion of an enzyme in a polymer network requires the synthesis of polymeric matrix in the presence of the enzyme. The

physical forces are not enough to retain the enzyme so an additional covalent attachment is often required.
Cross-linking of enzyme aggregates is used to prepare carrierless macroparticles. The loss of activity is inevitable due to the difficult accessibility of some of the enzyme situated deeply within the carrier pores, inaccessible to the substrate. However, this approach offers clear advantages: highly concentrated enzyme activity in the catalyst, high stability and low production costs owing to the exclusion of an additional carrier [40,41].

From literature, many techniques were used for chitinase and laccase immobilisation [37,42].
Chitinases were immobilised on silica gel by physical adsorption, on chitin and chitosan by covalent binding, on cellulose and Amberlite by ionic bonding. The obtained results show that chitosan, Amberlite and chitin had the highest immobilisation yield and the immobilisation on chitosan beads increases the activity of enzyme immobilised compared to the free enzyme [43,44]. In addition it was discovered that the immobilisation of chitosanase in chitin powder by cross-linking improves the enzyme properties [45].
Chitinase was also immobilised on calcium alginate, agar-agar, magnetic nanoparticles and silica gel beads and the immobilised chitinase expressed higher stability compared to the free one. It is an important factor for industrial applications [42,46].

Laccase was immobilised on Amberlite by covalent binding, the immobilised biocatalyst displays an improved thermal and storage stability paired with a good performance for the reusability [47]. Silica-based supports are widely studied for the immobilisation of laccases. The mesoporous silica materials act as good carriers for adsorption due to their pore size ordered structure, high surface area and high thermal stability. Good results were obtained immobilising laccases on mesoporous silica by physical adsorption and covalent bonding [48].
A wide variety of supports such as cellulose, agarose, collagen, inorganic carriers like glass, silica, metallic nanoparticles of gold, silver are widely used for laccase immobilisation [49].

The type of support material used plays a crucial role in the immobilisation process due to the strong effect of these materials on the properties of the produced catalytic system. The main required features of support materials for effective enzyme immobilisation products are: thermal and chemical stability, insolubility under reaction conditions, high affinity to enzymes, regeneration and reusability, availability and less price, presence of reactive functional groups and biocompatibility [50,51].
The support structure and immobilisation technique are major factors limiting the immobilisation process. Many techniques and carriers for immobilisation have been developed over the years; however, there is no universal method of immobilisation or ideal support for all enzymes and applications. Both have advantages and disadvantages, which need to be balanced through the optimisation process [52].

In this thesis, magnetic nanoparticles and chitosan beads as supports were investigated for the immobilisation of laccase and chitinase. The aim of the research was to optimize the immobilisation process in order to have advantages in the industrial application of these enzymes.

1.5 Magnetic nanoparticles

Nanoscience is one of the most important research in modern science. The use of nanoparticles offers major advantages due to their unique size and physicochemical properties. In fact, before focusing on the use of nanoparticles as a support for immobilisation, it is necessary to analyse their characteristics.

1.5.1 Physicochemical properties of magnetic nanoparticles

The term “nanoparticles” refers to materials with at least one dimension between approximately 1 and 100 nanometers (nm). Magnetic nanoparticles Fe_3O_4 (MNPs) are a class of nanoparticles that can be manipulated using magnetic fields [53].

Five basic types of magnetism can be described: ferromagnetism, paramagnetism, diamagnetism, antiferromagnetism and ferrimagnetism. In ferromagnetic materials, an atom has a net magnetic moment due to unpaired electrons. The material is composed of domains each containing large numbers of atoms whose magnetic moments are parallel producing a net magnetic moment of the domain that points in some direction. The magnetic moments of the domains are randomly distributed giving a zero net magnetic moment on the material. When the ferromagnetic material is placed in a magnetic field, the magnetic moments of the domains align along the direction of the applied magnetic field forming a large net magnetic moment.
In paramagnetic materials, an atom has a net magnetic moment due to unpaired electrons but magnetic domains are absent. When the paramagnetic material is placed in a magnetic field, the magnetic moment of the atoms aligns along the direction of the applied magnetic field forming a weak net magnetic moment.
In diamagnetic materials, atoms have no unpaired electrons, which results in zero net magnetic moment. These materials display a very weak response against the applied magnetic field due to the realignment of the electron orbits when a magnetic field is applied.
Antiferromagnetic materials are compounds of two different atoms that occupy different lattice positions. The two atoms have magnetic moments that are equal in magnitude and opposite in direction, which results in zero net magnetic moment.
Ferrimagnetic materials, such as magnetite Fe_3O_4, are also compounds of different atoms residing on different lattice sites with antiparallel magnetic moments. However, in these materials, the magnetic moments do not cancel out since they have different magnitudes which result in a net spontaneous magnetic moment [54].

An important aspect of magnetic nanoparticles is their surface. As the size of the particles decreases, the ratio of the surface area to volume of the particle increases. For nanoparticles, this ratio becomes significantly large causing a large portion of the atoms to reside on the surface compared to those in the core of the particle.

The large surface-volume ratio of the nanoparticles is the key factor to the physical, chemical and mechanical properties compared to those of the corresponding bulk material [55].
Furthermore, it was shown that the magnetic moment per atom and the magnetic anisotropy of nanoparticles could be different than those of a bulk specimen. It is well established that bulk ferrimagnetic material is composed of small regions, called magnetic domains. In each domain, the magnetic moments of atoms are aligned in one direction giving a net magnetization of each domain. The directions of magnetization of the domains are different. Hence the net magnetization of a magnetic material resulted from the addition of the different magnetization of all domains. It was found that magnetic domains in ferrimagnetic crystals have a minimum size, around 100 nm, below which the ferrimagnetic material cannot split up further into domains and are called single domain particles. Thermal energy plays a major role in the magnetic instability of single domain magnetic particles [56].

1.5.2 Magnetic nanoparticles synthesis

MNPs of different types and sizes are now being synthesized via several physical and chemical methods. The most common methods including co-precipitation, hydrothermal synthesis, thermal decomposition, microemulsion and sonochemical synthesis can all be directed to the synthesis of high quality iron oxide nanoparticles [57].
The co-precipitation technique is probably the simplest and most efficient chemical pathway to obtain magnetic particles. Iron oxide nanoparticles are usually prepared by an aging stoichiometric mixture of ferrous and ferric salts in aqueous medium.

$$Fe^{3+} + Fe^{2+} + 8OH^- \rightarrow Fe_3O_4\downarrow + 4\ H_2O \qquad (1)$$

According to the thermodynamics of this reaction, complete precipitation of Fe_3O_4 should be expected at a pH between 8 and 14, with a stoichiometric ratio of 2:1 (Fe^{3+}/Fe^{2+}) in a non-oxidizing oxygen environment. Magnetite (Fe_3O_4) is not very stable and is sensitive to

oxidation because it is transformed into maghemite (γ-Fe_2O_3) in the presence of oxygen.
The main advantage of the co-precipitation process is that a large number of nanoparticles can be synthesized.
A wide variety of factors can be adjusted in the synthesis of iron magnetic nanoparticles to control the size, magnetic characteristics or surface properties. A number of studies have dealt with the influence of these different factors. The size and shape of the nanoparticles can be tailored with relative success by adjusting pH, ionic strength, temperature, nature of the salts (perchlorates, chlorates, sulfates and nitrates) or the Fe^{3+}/Fe^{2+} concentration ratio. The addition of chelating organic anions or polymer surface complexing agents during the formation of nanoparticles can help to control the size of magnetite [53,58].

It is a challenge to control the size, stability, shape, and dispersibility of nanoparticles in desired solvents. Magnetic iron oxide nanoparticles have a large surface to volume ratio and therefore possess high surface energies. Consequently, they tend to aggregate to minimize the surface energies. Moreover, the naked iron oxide NPs have high chemical activity and are easily oxidized in air, generally resulting in loss of magnetism and dispersibility. Therefore, providing proper surface coating and developing some effective protection strategies to keep the stability of magnetic iron oxide NPs is very important. The coating is designed to improve the stability and solubility of nanoparticles, increase their biocompatibility, target specificity, and to prevent agglomeration, oxidation, corrosion and toxicity [59].
A promising approach is coating magnetic nanoparticles with silica. It could shield the magnetic dipolar attraction between magnetic nanoparticles, favouring the dispersion of the nanoparticles in liquid media. Furthermore, due to the existence of many silanol groups, magnetic nanoparticles could have various functional groups. Finally, silica provides a chemically inert surface for magnetic nanoparticles in biological systems [60].

1.5.3 Application of MNPs on enzyme immobilisation

The development of nanotechnology has found employment in enzymatic immobilisation, especially the use of magnetic nanoparticles had gained significant attention due to strong magnetic properties, low toxicity and biocompatibility with biological materials [61].
Nanoparticles present a high specific area, meaning that more enzymes can be immobilised, because it increases the available attacking surface. Furthermore, their magnetic force allows them to easily separate the final product from the reaction environment by applying an external magnetic field (Figure 3).

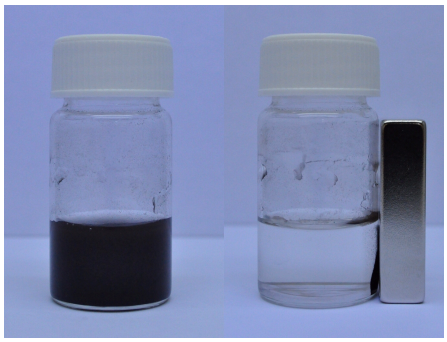

Figure 3 Attraction of magnetic nanoparticles applying external magnetic field

Compared with the conventional immobilisation methods, nanoparticle as support can be characterised by two main features: the composition, size and morphology of particles can be conveniently tuned by changing the reaction conditions and the uniform particles make it easy to perform the enzyme immobilisation on a large scale without using surfactants and toxic reagents. The methods developed for enzyme immobilisation on magnetic nanoparticles mainly include physical immobilisation and covalent conjugation.
Physical immobilisation can be considered the simplest functionalization method employed in protein immobilisation, as it may be easily carried out by just dipping the material into a solution containing the target biomolecules, and no additional coupling reagents, surface treatment and protein modification are required. Physical immobilisation is simple and mild, this method generally involves comparatively weak interactions such as electrostatic interactions, hydrogen bonds, van der Waals forces and hydrophobic interactions, and the binding stability of

adsorbed species is highly affected by environmental conditions (pH, temperature, ionic strength and enzyme concentration).
Covalent immobilisation is particularly attractive, as it could be carefully regulated with specific functional groups to bind to proteins. Several immobilisation protocols using covalent binding have already been developed and employed in enzyme immobilisation [62].
For example, Laccase, aminoacylase and lipase were immobilised via covalent bonding to magnetic nanoparticles coated with 3-(aminopropyl)triethoxysilane (APTES) and glutaraldehyde. Coupling agents such as glutaraldehyde are often utilized to covalently cross-link the modified magnetic nanoparticles and enzymes because their functional group e.g.; aldehyde group can interact with both functional groups of the modified magnetic nanoparticles and proteins [63–66].

1.6 Chitosan supports

The efficiency of the enzymatic immobilisation system depends on the properties of support material and enzyme. A number of desirable characteristics should be common to any support, such as high affinity to proteins, hydrophilicity, availability of functional groups for reactions with enzymes or for chemical modification, rigidity and mechanical stability, easy preparation, chemical and thermal stability. Furthermore, for pharmaceutical, medical and food applications, no-toxicity and biocompatibility are also required. In addition, to respect the environment, the support should be biodegradable and to make the system industrially applicable the material should be inexpensive.
So many characteristics seem difficult to have many materials that have been designed for enzymatic immobilisation, organic or inorganic, natural or synthetic. Chitosan has many of the above mentioned characteristics.
Chitosan is a natural polysaccharide, so it is biocompatible, biodegradable, physiological inertness and non-toxic. It is obtained at a relatively low cost from shells and shellfish, waste of the seafood processing industry. Chitosan has reactive amino and hydroxyl groups, amenable to chemical modifications. In addition, amino groups make chitosan a cationic polyelectrolyte, one of the few found in nature. This

characteristic gives important properties: chitosan aggregates with polyanionic compound, it is soluble in aqueous acidic media (pH < 6.5) and when dissolved has a high positive charge on $–NH_3^+$ groups that adhere to negatively charged surfaces [67].

Chitosan is often used as support for enzyme immobilisation [68–72].
As enzyme immobilisation supports chitosan is used in the form of powder, flakes and gels. To prepare the chitosan gel need to dissolve it in dilute solutions of most organic acids, such as formic, acetic, tartaric and citric acids, to form viscous solutions that precipitate upon an increase in pH and by the formation of water-insoluble ionotropic complexes with anionic polyelectrolytes. In this way, chitosan gels in the form of beads, membranes, coatings, capsules, fibres, hollow fibres and sponges can be manufactured [73].
The methods of chitosan gel preparation described in the literature can be broadly divided into four groups: [74,75]

i. Solvent evaporation method
   The method is usually applied for the preparation of membranes and films. The solution of chitosan is cast onto a plate and allowed to dry at an elevated temperature of about 65 °C. Then membrane/film is neutralized with a dilute NaOH solution and crosslinked to avoid disintegration. Enzymes could be immobilised on the film/membrane by adsorption, covalent binding or inclusion. Spray drying is a variant of the solvent evaporation method allowing the preparation of beads smaller in size than those prepared with the other methods [76].

ii. Neutralization method
   This technique is used to obtain chitosan spherical beads of different sizes. These are obtained by adding a chitosan solution dropwise to a NaOH solution. The enzyme could be immobilised with the common methods: adsorption, covalent binding or inclusion [77].

iii. Crosslinking method

In this method, a chitosan solution is mixed with a crosslinking agent to obtain a gel.

The crosslinker is a bifunctional agent, it has two functions: crosslinking and activation, so the immobilisation of the enzyme on such prepared gels does not need chemical activation.

Glutaraldehyde is the common crosslinker used, due to its reliability and ease of use, but more importantly, due to the availability of amino groups for the reaction with glutaraldehyde not only on enzymes but also on chitosan [78].

iv. Ionotropic gelation method

The method is utilized chiefly for the preparation of gel beads, which is achieved by adding an anionic polyelectrolyte solution dropwise into an acidic chitosan solution. Chitosan has a cationic polyelectrolyte nature then spontaneously forms water-insoluble complexes with anionic polyelectrolytes. The anionic poly-electrolytes used include alginate, molybdate, carrageenan, xanthan, various polyphosphates and sulfates or enzymes themselves. Enzyme immobilisation is achieved by preparing an enzyme-containing anionic polyelectrolyte solution prior to gelation. The enzyme is immobilised by inclusion in the interior of the beads/capsules [79,80].

In this thesis the production of chitosan beads/Macro-Spheres (CMS) following the neutralization methods was carried out. The presence of amino groups in chitosan allows the binding of the linker and then of the enzyme. Most enzymes, such as trypsin, laccase and peroxidase have been already immobilised on CMS with successful results.[81–83] For chitinases the immobilisation process needs to be optimized because many articles use chitinase immobilised on CMS but a decrease of activity after the reuses was observed [84,85].

1.7 Enzymatic synthesis of Melanin

In paragraph 1.3 was reported that laccases are oxidases that contain several copper atoms and catalyse single-electron oxidations of phenolic compounds with concomitant reduction of oxygen to water. Laccases are involved in various biosynthetic processes contributing to carbon recycling in land ecosystems and the morphogenesis of biomatrices, wherein low molecular weight naturally occurring phenols serve as key enzyme substrates. Laccase catalysed processes yield several types of biopolymers, including those of cuticles, lignin, polyflavonoids and melanin pigments, using natural mono- or poly-phenols as building blocks. Notably, such synthetic pathways can also reproduce physicochemical properties (e.g. those of chromophores, and radical-scavenging, hydration and antimicrobial activities) found in natural biomaterials [86].
This part of the thesis is focused on the use of laccase to produce different melanin pigments. The latter have been compared with melanins from different sources and characterised using EPR spectroscopy.

1.7.1 Melanin

Melanin is a biopolymer present in living organisms and plants, especially it is found in the skin and hair of mammals, in the ink of sepia in bacteria, birds and insects.
Melanin is a pigment characterised by unique properties. It is easy and cheaply available, biocompatible, biodegradable, it has strong relevance in the production of biomaterials, owing to the need for biomaterials with no toxicity [87].
Melanin has the ability to absorb radiation, quench and scavenge excited molecules. This is why melanin plays an important role in protecting human skin against damage caused by UV-visible radiation [88,89].
Among its biological functions are thermoregulation, anti-oxidant and chelating action, antibiotic function. Melanin has chelating properties through the anionic functions such as the carboxyl and deprotonated

hydroxyl groups. The antibiotic properties are due to the presence of nucleophilic groups such as thiols (-SH) and amino groups (-NH_2) [90].
In plant, melanin provides mechanical strength and protection from damage [91].
In human, this molecule plays an important role through its special properties and functions affecting general health, including photoprotective and immunological action. Recently, it has been demonstrated that melanin modulates cytokine production, stimulates lymphoid tissue and antibody production. Its antioxidant, anti-inflammatory, immunomodulatory, radioprotective, hepatic, gastrointestinal and hypoglycaemic benefits have only recently been recognized and studied. Finally, melanin can also be involved in nerve system protection. For instance, the melanin present in the brain (neuromelanin), specifically in the substantia nigra, helps neurons to manage the toxic presence of iron and other metals, through metal induced oxidative stress, promoting neuronal survival. This melanin plays a protective role in the skin as neuromelanin plays against several harmful factors to neurons. It is also associated with certain disorders of the nervous system such as Parkinson's disease [92,93].

Furthermore, Melanin has special chemical-physical properties essential to its function. Melanin appears as a black solid and is almost insoluble in the aqueous and organic solvents. It presents a highly negative surface, which confers stability to the molecules by electrostatic repulsion [94].
Regarding the UV-visible absorption spectrum, melanin resembles more an inorganic semiconductor material than an organic typical chromophore. In addition, the spectrum changes during the formation of the polymer. In fact, it evolves during the oxidation and agglomeration of the melanin precursors, associated with the formation of new cross-links [95].
Melanin has the ability to convert the absorbed UV light radiation into heat [96]. The ability to absorb radiation will quench and scavenge excited molecules, promoting a photoprotective effect in melanin pigments. This characteristic is reflected in the protection of human skin by the melanocytes against UV damage [88].

Another important property is the radical scavenging and antioxidant activity that is due to the existence of DHICA monomers, by transfer of H atoms. This characteristic is attributed to the chemical structure of the monomers, DHICA being less stable and less aggregated tends to react with reactive oxygen species (ROS) generated by physiological reactions [97].
Moreover, melanin holds strong electrical and photo-conductivity. The indolic structure of melanin and the electronic delocalization are thought to be responsible for its electrical conductive properties under specific conditions of humidity, temperature and electrical fields. On the other hand, photoconductivity, which under UV or visible light absorption decreases the resistance, is influenced by the oxidation of hydroxyquinones to semiquinones, releasing mobile protons. These properties are owed to the free radicals of the quinones oxidation, which can reduce or oxidize metals [98]. Melanin is a promising coating for material technology and in the field of optoelectronics, as a large proportion of the new melanin applications rely on their efficient photon-photon coupling [99].

Melanin is a heterogeneous biopolymer, the molecular structure has not yet been univocally defined because it varies depending on polymerization conditions. In fact, it has a high molecular weight due to the oxidizing polymerization of phenolic or indolic compounds.

1.7.2 Melanogenesis

The biosynthetic process of melanin is called melanogenesis, it is a complex pathway involving a combination of enzymatic and chemical catalysed reactions. This process produces two types of melanin: eumelanin and pheomelanin formed by the conjugation of cysteine or glutathione (Figure 4) [100].
Melanogenesis is started with the oxidation of tyrosine to dopaquinone (DQ) by an oxidative enzyme called tyrosinase (TYR). The quinone produced will serve as a substrate of eumelanin and pheomelanin synthesis. Then, DQ undergoes intramolecular cyclization to produce indoline, leukodopachrome (cyclodopa). The redox reaction between

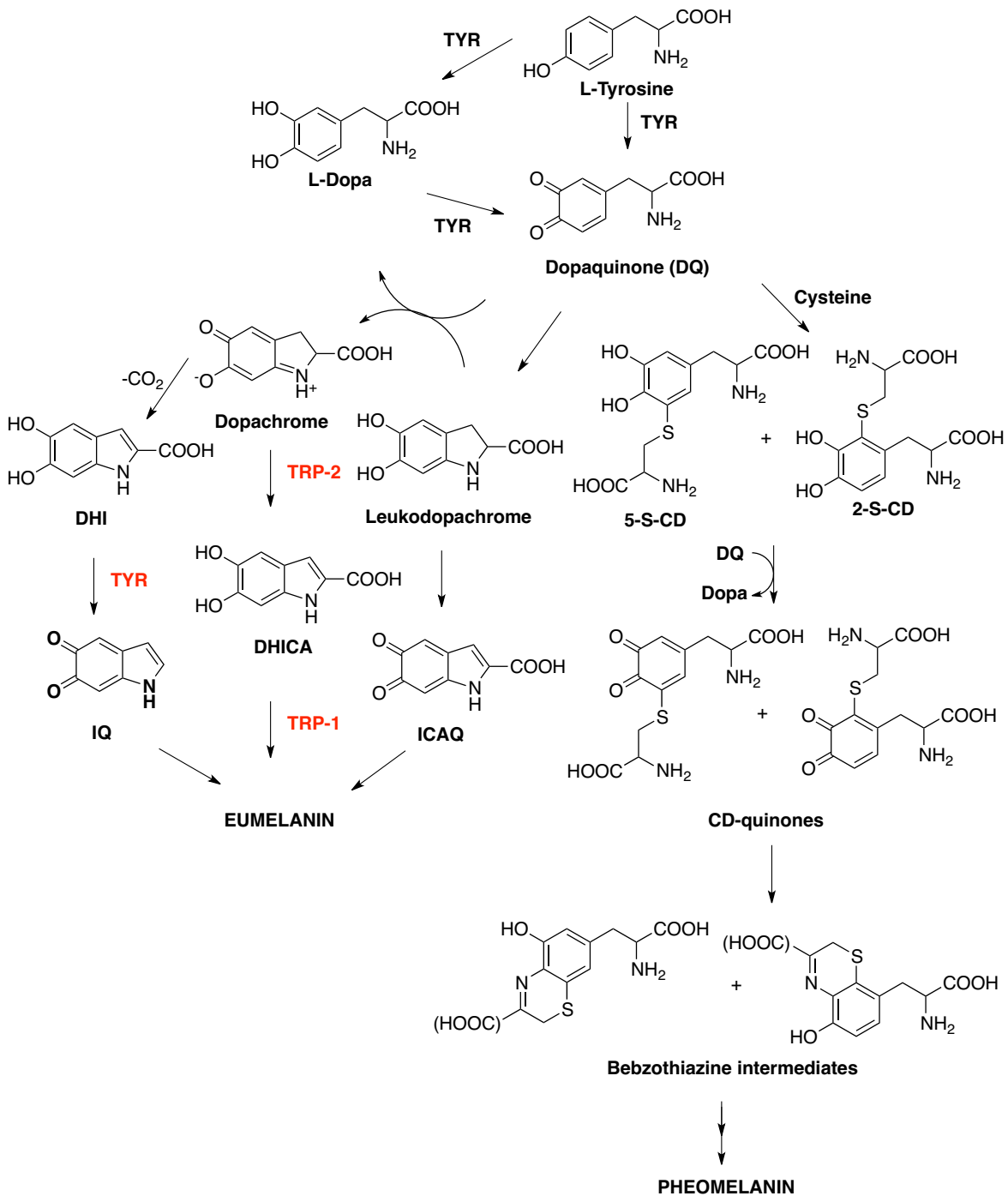

Figure 4 Melogenesis process: eumelanin and pheomelanin production. (Tyr: Tyrosinase; Trp-1: Tyrosinase-related protein-1; Trp-2: Tyrosinase-related protein-2; DQ: dopaquinone: L-Dopa: L-3,4-dihydroxyphenylalanine; DHICA: 5,6-dihydroxyindole-2 carboxylix acid; DHI: 5,6-dihydroxyindole; ICAQ: indole-2-carboxylic acid-5,6-quinone; IQ: indole-5,6-quinone; CD: cysteinyl-dopa; 5-S-CD: 5-S-cysteinyl-dopa; 2-S-CD: 2-S-cysteinyl-dopa.)

leukodopachrome and DQ gives rise to dopachrome and L-3,4-dihydroxyphenylalanine (L-DOPA), which is also a substrate for tyrosinase and can be oxidized to DQ. Dopachrome is gradually modified through reactions that lead to the formation of dihydroxyindole (DHI) and dihydroxyindole-2-carboxylic acid (DHICA). The following step is catalysed by TRP-2 (Tyrosinase-related protein-2), now known as dopachrome tautomerase (DCT). Finally, DHI and DHICA are oxidized by TRP-1 (Tyrosinase-related protein-1) to eumelanin. Alongside, in the presence of cysteine or glutathione, DQ is converted to 5-S-cysteinyl-dopa or glutothionyldopa. Consequently, their oxidation gives benzothiazine intermediates and at the end pheomelanin [101].
Three are the enzymes involved in the melanogenesis process, TYR, TRP-1 and TRP-2, but tyrosinase plays the most important role [102].
Tyrosinases, also called monophenol monooxygenases, are type 3 copper proteins with two copper ions in the active site. They manifest two catalytic properties: monooxygenase and oxidase activity. These actions reflect the oxidation states of the active center. They catalyse the conversion of monophenols into *o*-diphenols, followed by the oxidation of the *o*-diphenols to the corresponding quinone derivates [103,104].

1.7.3 Types of Melanin

As mentioned above the structure of melanin has not been characterised because of its heterogeneity. To better comprehension of the melanin structure, should be important analyse the classification of melanin according to the source: animal melanin, plant melanin, fungal melanin and bacterial melanin (Figure 5).

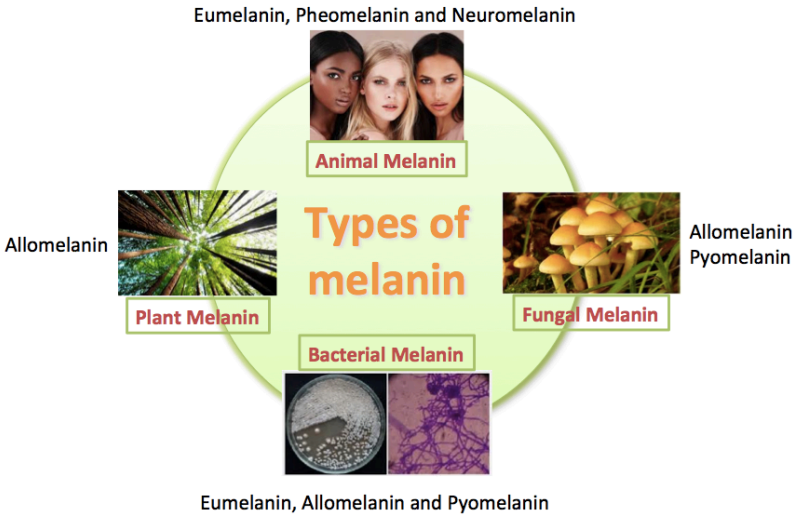

Figure 5 Classification of melanin according to the source

I. Animal melanin

Melanin is the main pigment responsible for the various pigmentations found in animal and human skin, hair and eyes. Basically, most of the melanins are dark, from black to brown, but other melanins are reddish or yellowish. According to that, animal melanin is divided into two large groups: eumelanin and pheomelanin. [105,106] Eumelanin provides primarily dark colors, from brown to black. Eumelanin structure has been hampered because it is difficult to study due to its insolubility and resistance. Due to the unavailability of crystallized melanin, the structure could not be ascertained by the most classical physical methods such as X-ray diffraction. Pheomelanin is more treatable than eumelanin because can be dissolved in alkali media. The color of pheomelanin is yellowish or reddish, and it is found in relatively large quantities in red hair, freckles and feathers of fowls and other birds. The main difference of eumelanin in chemical terms is the presence of sulfur. Melanin is also found in certain regions of the brain and adrenal gland of some mammals, this particular melanin is called neuromelanin, it is a dark polymer pigment produced in specific populations of catecholaminergic neurons in the brain, mostly sited in the *substantia nigra* and in lower proportion in the *locus coeruleus*. Neuromelanin is a mixture of pheomelanin and eumelanin. Neuromelanin granules should

have pheomelanin in the core and eumelanin in the surface, which is compatible with occasional exhaustion of glutathione or cysteine reduction system during neuromelanin formation [107]. Furthermore, in mammals, melanin is formed even in some other tissues different from the skin, eye, inner ear, and brain, as in the adipose tissue [108]. Aside from mammals, bird feathers contain eumelanin and pheomelanin and the relative amounts of each pigment differ with the avian species [109]. Melanin is also found in reptiles, amphibians, and fish. These animals can change color relatively rapidly to camouflage themselves against changing backgrounds so that melanin is more versatile and offers hue due to the existence of chromatophores and iridophores in addition to melanocytes [110]. The ink in the cuttlefish contains a special type of melanin called sepiamelanin. This melanin is mostly eumelanin, as it is formed by an irregular heteropolymer of indole and carboxylated pyrrolic units with some associated protein [111]. In insects, melanins are present to protect their soft bodies by a process called sclerotization [112]. The main precursor for that process is N-acetyldopamine, which is derived from the amino acid L-tyrosine, so this melanin should be considered as a special type of eumelanin [113].

II. Plant melanin

The presence of nitrogen is important for plant growth. According to that, the amino acid L-tyrosine is not used for the synthesis of plant melanin. They employ some phenol nitrogen-free precursors, such as catechols, dihydroxynaphthalenes or other types of dihydroxybenzenes to carry out this part of its secondary metabolism. In general, the obtained melanin is a polymer without nitrogen and is generically named allomelanin. In plants, the most common precursor is just catechol, so the melanin formed is also named catechol-melanin. and the enzymatic system involved in the synthesis is named catechol oxidase [114,115].

The color of allomelanin is always from dark brown to totally black, and its structure depends on the nature of the main unit

oxidized. Some vegetables use just normal catechol, but others use different catecholic acids such as caffeic, protocatechuic, chlorogenic or gallic acids. According to that, the melanin pigment is a polymer derived from these catechols and the corresponding quinones formed by the action of catechol oxidases [116].

III. Fungal melanin

Fungal melanin is quite abundant and appears in the cell wall [117]. The precursors and the nature of the corresponding melanin structure show variability. The first characterisations suggested catechol precursors form allomelanin devoid of nitrogen by similarity to plant melanins. However, the precursor identified was not catechol, but hydroxylated naphthalene-derived molecules. In this way, a new subtype of allomelanins was described, the DHN-melanins (dihydroxynaphthalene melanin). This type of melanin is quite common in ascomycetous and some imperfect fungi. DHN-melanine has also been identified in the yeast. In basidiomycetes, melanin is formed from a benzoquinone obtained by the action of tyrosinase on the precursors, gamma-glutaminyl-4-hydroxybenzene (GHB). This synthesis could be considered specific to mushrooms and different from all other melanin pigments. Other basidiomycetes as *Cryptococcus neoformans* are also able to synthesize pyomelanin derivated from a fungal metabolite, homogentisic acid (HGA) [118]. The possibility to synthetize two different types of melanin depending on the environmental conditions. This characteristic was also observed in *Aspergillus fumigatus*, which is able to form DHN-melanin and pyomelanin starting *L*-tyrosine through homogentisic acid and in *Aspergiullus nidulas* that forms the DHN-melanin and DOPA-melanin [119–121].

IV. Bacterial Melanin

In a great number of bacterial species were found melanin pigments characterised by black or dark brown colors. *Streptomices* species are considered the model for the study of

the tyrosinase, its structure, catalytic mechanism, regulation and its expression. Simultaneously, they were used to analyse the final product, melanin [122,123]. In *Streptomices*, melanins contain nitrogen and their structure is similar to animal eumelanin. However, there are also bacteria such as *Azotobacter* that can form allomelanin from catecholic precursors [124]. Some bacteria are able to produce DHN-melanin and others as *Pseudomonas* are able to produce pyomelanin from homogentisic acid, in fact, was observed that some bacteria synthesize pyomelanin in response to specific physiological conditions that are stressful for theirs. Under those conditions, there is an accumulation of homogentisic acid due to the low activity of homogentisate dioxygenase. Consequently, homogentisic is oxidised and pyomelanin is formed [116].

1.7.4 Melanin characterisation by EPR Spectroscopy

Melanin is an amorphous organic polymer with numerous intermediate free radicals trapped in its structure. These paramagnetic centers are responsible for the special paramagnetic properties of melanin. For this Electron Paramagnetic Resonance (EPR) became an important spectroscopic technique to study and characterise this polymer.
In fact, EPR spectroscopy is useful to identify and study chemicals that have one or more unpaired electrons, though their paramagnetic properties is possible to identify their structure and characteristics [125].
Moreover, EPR spectroscopy can be considered as one of the most advantageous methods to investigate melanin and to estimate the concentration of pheomelanin and eumelanin.
Investigation of synthetic (5-S-cysteinyldopa) polymer of pheomelanin showed that the EPR spectra of free radicals in cysteinyldopa and dopa-melanin are clearly different. The dopa-melanin radicals appear to be ‘O-C-C-O’ semiquinones (Figure 6,a) whereas cysteinyldopa melanin radicals are ‘O-C-C-N’ semiquinonimines (Figure 6,b). Consequently, ‘O-C-C-O’ semiquinones give singlet-shaped EPR spectra. This is caused by interactions of unpaired electrons with oxygen nucleus resulting in no hyperfine splitting, whereas the interaction between an

unpaired electron and nitrogen ^{14}N nucleus (I=1) gives a triplet-shared EPR spectrum [126,127].

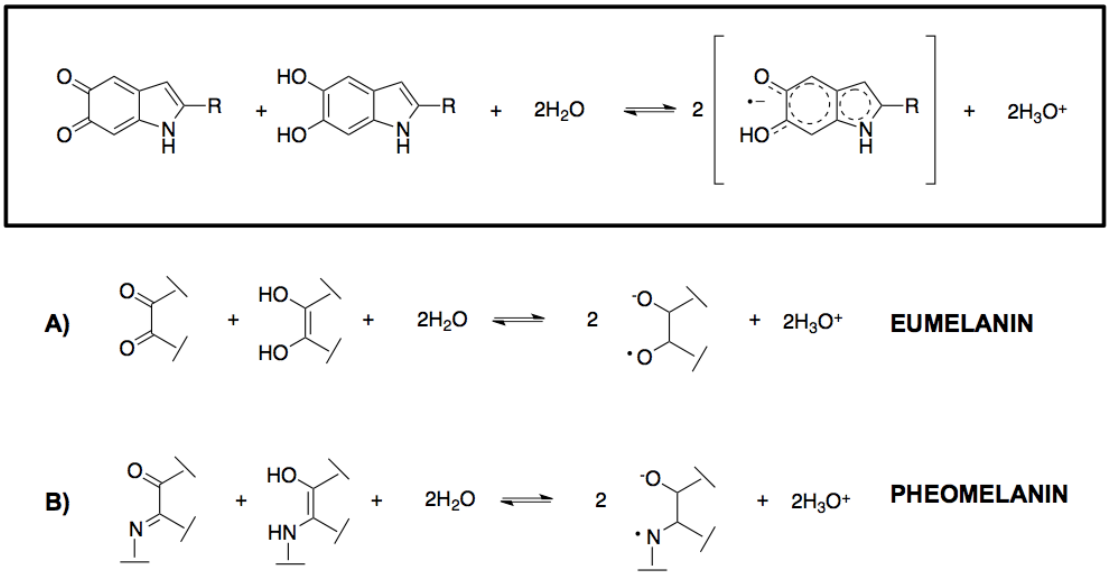

Figure 6 Formation of semiquinone radicals in melanin. a): eumelanin b): pheomelanin

1.7.5 EPR Spectroscopy

Spectroscopy is the measurement and interpretation of the energy differences between the atomic and molecules states to collect information about the identity, structure and dynamics of the sample analysed.

These energy differences expressed by ΔE have an important relationship with the absorption of electromagnetic radiation. According to Planck's law, electromagnetic radiation will be absorbed if:

$$\Delta E = h\nu \qquad (2)$$

where h is Planck's constant and ν is the frequency of the radiation.

The absorption of energy causes a transition from a lower energy state to a higher energy state. In conventional EPR spectroscopy, ν is maintained constant and the magnetic field H is varied until the ΔE is

matched by the frequencies at which absorption occurs, through the so-called “resonance condition”.

$$h\nu = g\beta H$$

For EPR experiments, radiation in the gigahertz range (GHz) with a wavelength of a few cm is used [128].

An isolated electron, without any outside forces, has an intrinsic angular moment called “spin”. An electron has a charge and the angular motion of this charge generates a magnetic field then it acts like a little bar magnet or magnetic dipole with a magnetic moment indicated with μ (Figure 7,a).
EPR spectroscopy studies the energy differences due to the interaction of unpaired electrons in the sample with a static magnetic field. This effect is called the Zeeman Effect. The magnetic field, B_0, produces two energy levels for the magnetic moment of the electron. The unpaired electron will have a state of lower and highest energy when the magnetic moment is aligned with the magnetic field (Figure 7,b).

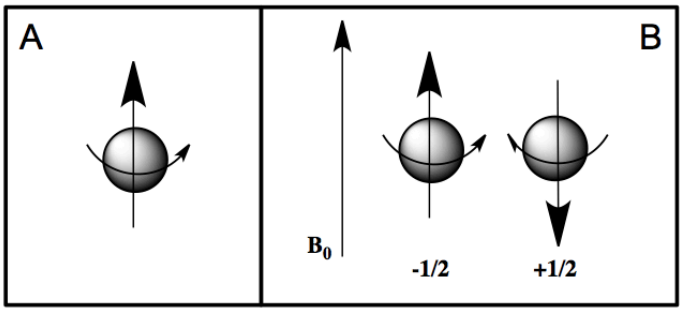

Figure 7 a) Electron spin and magnetic moment of unpaired electron; b) Minimum and maximum energy orientation of magnetic moment respect to magnetic field B_0

The two states are labelled by the projection of the electron spin, m_s, on the direction of the magnetic field. Because the electron is a spin 1/2 particle, the parallel state is designed as m_s= +1/2 and the antiparallel state is as m_s= +1/2. The energy of each orientation is the product of μ and B_0. For and electron $\mu = m_s g_e \beta$, where β is a conversion constant

called the Bohr magneton and g_e is the spectroscopic g-factor of the free electron and equals 2.0023192778 ($\approx$ 2.00).
As described in figure 8, there are two energy levels for the electron in a magnetic field.
The distance between Zeeman levels is characteristic of the particular type of paramagnetic centres and is expressed by g-factor ($g= h\nu/\beta B_0$).
The position of the middle of EPR spectrum provides information about g-value and on the type of paramagnetic centre, while the quantitative information is delivered by the field under the curve of adsorption of microwaves (the internal intensity of the signal).

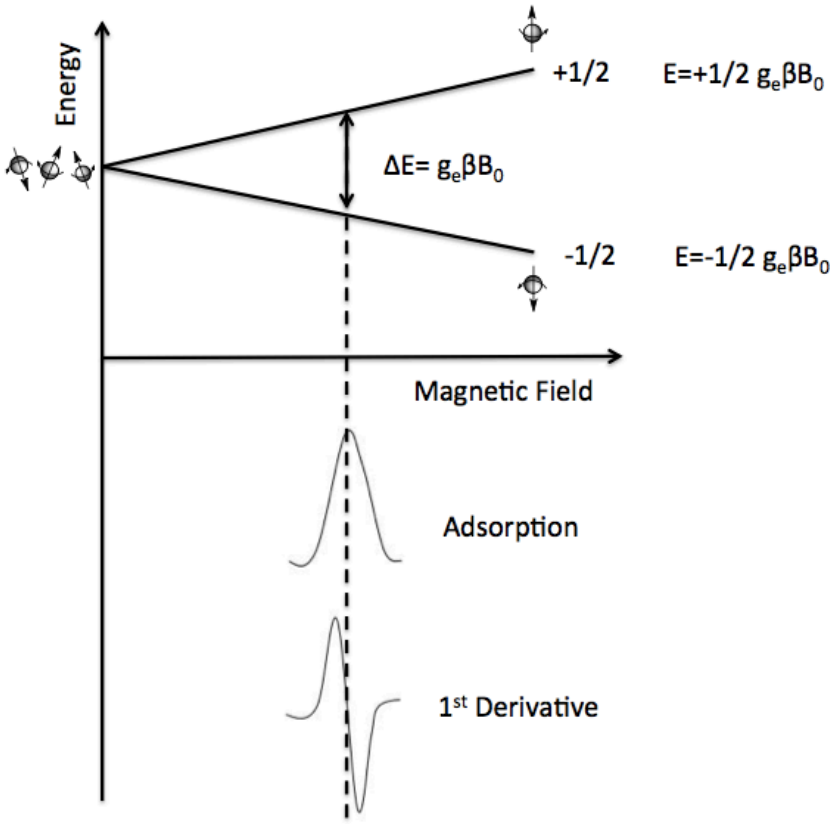

Figure 8 Zeeman splitting of the energy levels of the system of unpaired spins in the external magnetic field. Below the absorption curve and its first derivative.

In real systems, electrons are normally associated with one or more atoms. There are several important consequences of this:

i. An unpaired electron can gain or lose its angular momentum, which can change the value of *g*-factor. For every paramagnetic molecule, there exists a unique axis system called the principal axis system. The *g*-factor measured along these axes are called the principal *g*-factors and are labeled g_x, g_y and g_z.
ii. Systems with multiple unpaired electrons experience electron-electron interactions that give rise to 'fine' structure. This is realized as zero field splitting and exchange coupling and can be large in magnitude.
iii. The magnetic moment of a nucleus with a non-zero nuclear spin will affect any unpaired electrons associated with that atom. This leads to the phenomenon of hyperfine coupling, splitting the EPR resonance signal into doublets, triplets and so forth. Additional smaller splittings from nearby nuclei is called "superhyperfine" coupling.
iv. Interactions of an unpaired electron with its environment influence the shape of an EPR spectral line.
v. These effects in an atom or molecule may not be the same for all orientations of an unpaired electron in an external field. This anisotropy depends upon the electronic structure of the atom or molecules in question, and so can provide information about atomic or molecular orbital containing the unpaired electron.

With the intensity of the applied magnetic field increasing, the energy difference between the energy levels widens until it matches with the microwave radiation, and results in the absorption of photons. This is the fundamental basis for EPR spectroscopy. EPR spectrometers typically vary the magnetic field and hold the microwave frequency. EPR spectrometers are available in several frequency ranges (Table 2).
EPR experiments often are conducted at X and, less commonly, Q bands, but the low spectral resolution over *g*-factor at these wavebands limits the study of paramagnetic centers with comparatively low anisotropic magnetic parameters.

Table 2 List of microwave frequencies commonly available in EPR spectrometers

Microwave Band	Frequency (GHz)
L	1.1
S	3.0
X	9.5
Q	35
W	90
J	270

Continuous wave (CW) are recorded by putting a sample into a microwave irradiation field of constant frequency and sweeping the external magnetic field B_0 until the resonance condition is fulfilled.
In pulse EPR the spectrum is recorded by exciting a large frequency range simultaneously with a single power microwave pulse of a given frequency at constant magnetic field B_0.
Most EPR applications still make use of continuous wave methods as the recording and interpretation of pulse EPR spectra requires sophisticated technical equipment and a more advanced theoretical background. A significant advantage of CW EPR with respect to the pulse methods is the higher sensitivity. A further limitation of pulse EPR is also the low measuring temperatures imposed by the short relaxation of the transverse magnetization involved in pulse experiments, especially for transition metal ions. CW EPR spectra on the other hand can be recorded at room temperature for a large number of spin systems, including radicals and transition metal ions. The additional information about weakly coupled nuclei and relaxation properties of the spin system that can be obtained by manipulating the spins with sequences of MW pulses explains on the other hand the efforts put into the development of new pulse methods. In fact, CW and pulse EPR are complementary and only the application of both gives a reliable picture of the spin system [129,130].

ENZYMATIC IMMOBILISATION

This chapter reports the development of immobilisation systems for laccase and chitinase. The preparation of high-performance and economically-feasible biocatalysts with improved stability and reusability was the object of this research. Magnetic nanoparticles Fe_3O_4 (MNPs) were chosen as support for both enzymes used. Chitinase was successfully immobilised on MNPs using the traditional methods. The magnetic nanoparticles were functionalised with amino groups using (3-aminopropyl) triethoxysilane (APTES) and then glutaraldehyde to allow the covalent immobilisation of the enzymes. Different were the results for laccase, which is characterised by a different catalytic mechanism.

Laccase catalyses the formation of stable radicals which seem to be adsorbed by magnetic nanoparticles, making the immobilization process not usable. This behaviour was observed with ABTS, the standard compound used to test the laccase activity. In this context, the MNPs synthesis and immobilisation process were modified. Changing some synthetic parameters new magnetic nanoparticles (MNPs-2) were produced and compared to traditional magnetic nanoparticles (MNPs-1). MNPs-2 showed a better dispersion and consequently a smaller hydrodynamic diameter. The laccase was successfully immobilised by absorption and covalent methods and the activity test was carried out without any interference with the ABTS substrate.

The toxicity of MNPs-1 before and after laccase immobilisation was evaluated. The results show the lower toxicity of nanoparticles after the immobilisation.

Alternative support was studied for chitinase immobilisation. Chitosan beads/Macro-Spheres (CMS) were chosen as support due to their atoxicity and usability in food industry applications. Furthermore, their chemical structure characterised by amino groups of chitosan allows the covalent binding of the linker such as glutaraldehyde and genipin and then of the enzyme. The chitinase immobilised was used for the production of Chitooligosaccharides (COS), which are important in the biotechnological field due to their antioxidant and antimicrobial properties.

2.1 MNPs synthesis

Superparamagnetic nanoparticles Fe_3O_4 (MNPs) were synthetized using chemical co-precipitation of Fe^{3+} and Fe^{2+} ions. Two different methods were using which in the following text will be called MNPs-1 and MNPs-2:

1) MNPs-1: $FeCl_3 \cdot 6H_2O$ (2,335 g, 2 eq.) and $Fe(SO_4)_2(NH_4)_2SO_4 \cdot 6H_2O$ (1,863 g, 1 eq.) were dissolved in 50 ml ultrapure water and were left for about 30 minutes to bubble under nitrogen until the temperature reached 60 °C. Then 45 ml of a solution 1 M di NaOH was added. The reaction solution quickly changed colour and became black, the heat was turned off and was left to react under nitrogen for 1 hour. Afterwards, the Fe_3O_4 nanoparticles were separated from the reaction solution with a magnet and washed several times with ultrapure water until the pH solution became neutral. The nanoparticles were dried dried under N_2 flux.

2) MNPs-2: 1.62 g ferric chloride and 0.64 g ferrous chloride (ratio 2:1) were dissolved in 50 ml of bidistilled water and mixed in a flask with two necks under nitrogen. After 10 minutes, 3 ml of ammonia solution (NH_3OH 25%) was added drop by drop, a black precipitate was observed and left to react for 1 hour. Then, the nanoparticles were separated and washed with ultrapure water using several cycles of ultracentrifuge (cycle: 30000 rpm, 20 degrees and 1 hour). After that, the nanoparticles were freeze-dryer [131].

Table 3: Comparison between the MNPs-1 and MNPs-2 synthesis and nanoparticles characteristics

PARAMETER	MNPs-1	MNPs-2
Temperature	60°	25°
Fe^{2+} salt	$Fe(SO_4)_2(NH_4)_2SO_4 \cdot 6H_2O$	$FeCl_2$
Fe^{3+} salt	$FeCl_3 \cdot 6H_2O$	$FeCl_3$
Fe^{2+}/Fe^{3+} molar ratio	1:2	1:2
Precipitating agent	NaOH	NH_4OH
Using N_2 gas	yes	yes
Hydrodynamic diameter	**227 nm**	**49 nm**

MNPs-1 and MNPs-2 were synthetized by co-precipitation of ferric and ferrous ions. In the co-precipitation method, two strategies are involved: a short burst of nucleation occurs when the concentration of the species reaches critical supersaturation, and then, there is a slow growth of the nuclei by diffusion of the solutes to the surface of the crystal. To produce monodisperse iron oxide nanoparticles, these two stages should be separated; i.e., nucleation should be avoided during the period of growth [53].

The co-precipitation process depends mostly on parameters such as reaction temperature, pH, nature of salts, type of precipitant agent and Fe^{2+}/Fe^{3+} molar ratio. The parameters of synthesis were changed to study the effect of the correlation between those parameters and the nanoparticles size (Table 3).

The change in the reaction temperature can bring to control the size of magnetic nanoparticles. The average size and the distribution percentage size of Fe_3O_4 nanoparticles increase with the reaction temperatures due to the acceleration of chemical reaction of Fe^{2+} and Fe^{3+} ions [132–134]. MNPs-1 and MNPs-2 synthetized at 60°C and 25°C respectively did not report many differences in size but the lower temperature used for the synthesis, improved the distribution percentage size, obtaining a hydrodynamic diameter of 49 nm for MNPs-2.

Another factor affecting the size of magnetic nanoparticles is the Fe^{2+}/Fe^{3+} molar ratio. In both synthesis the ratio were 1:2 [135].

The presence of inert gas such as nitrogen is necessary for the production of magnetic nanoparticles because magnetite (Fe_3O_4) in presence of oxygen can be oxidized into maghemite (γ-Fe_2O_4) [53].

The precipitant agent plays another important role in the reaction system, NaOH was used for MNPs-1 and NH_4OH for MNPs-2.

NaOH has a high concentration of OH^- and the higher pH value, with the same concentration of alkali, will accelerate the reaction and lead to large particle size. On the contrary, NH_4OH releases OH^- gradually to make the particle size controllable and the process more stable [136]. In this context, NH_4OH favours a better dispersion of MNPs-2, however, no change in size has been observed.

The ionic strength is another effect that allows the control of size and dispersion of magnetic nanoparticles. The higher ionic strength of the solution causes a reduction of zeta potential at a constant pH, resulting in lower electrostatic stability and an increase of the hydrodynamic diameter of the particles [137].
The different nature of salts for MNPs-1 and MNPs-2 synthesis affects the ionic strength, MNPs-1 have a higher ionic strength that increases their hydrodynamic diameter.

2.2 MNPs characterisation

In order to test the stability of the dispersions of MNPs-1 and MNPs-2, several solutions with different pH (from 3 to 9) were prepared, the ζ-potential and size were measured for those samples (Figure 9). The surface charge of magnetic nanoparticles depends on the pH value. In an aqueous system, the surface is covered with groups of –FeOH. At lower pH (pH < isoelectric point of MNPs), the higher content of H^+ caused the protonation of OH and the formation of $–FeOH_2^+$. Instead, increasing the pH value (pH > isoelectric point of MNPs), the OH are deprotonated forming FeO^-, which gives a negative charge to the surface of the nanoparticles [138]. According to this, the z-potential of MNPs-1 showed a positive and negative charge before and after their isoelectric point. The different behaviour was observed for MNPs-2, that at high pH values they did not have a negative charge. This suggests the presences of NH_4^+ on the nanoparticles surface. It was assumed that during the synthesis of MNPs conducted under alkali conditions [131], the NH_4^+ from precipitating agent (NH_4OH) was attracted by $–OH^-$ of nanoparticles, giving them a positive charge. This interaction was reported by Unsoy et al. in the synthesis of chitosan coated iron oxide nanoparticles, where $–NH_3^+$ groups of chitosan were attracted by $–OH^-$ of iron oxide [139].
Another point that supports the hypothesis of the presence of NH_4^+ on the nanoparticles surface is the shift of isoelectric point. From the literature, The isoelectric point of MNPs-NH_2 shifts to higher pH values [140], instead, when negative charged groups such as $SO_4^=$ are

absorbed at the nanoparticles surface the isoelectric point shifts to lower pH values [141].

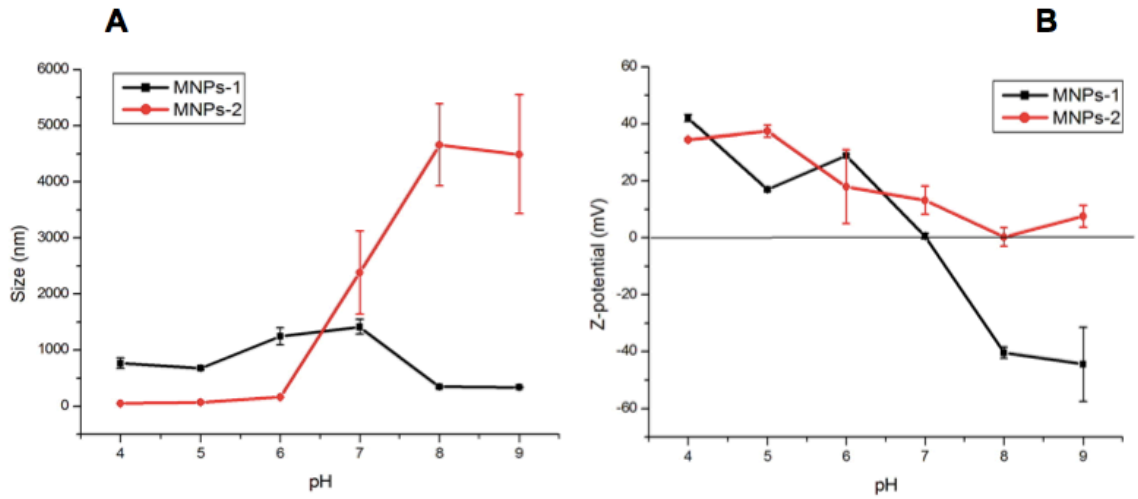

Figure 9 MNPs pH stability. A) Size comparison between MNPs-1 and MNPs-2 with different pH (from 4 to 9); B) ζ-potential comparison between MNPs-1 and MNPs-2 with different pH (from 4 to 9)

Morphology and size of nanoparticles were evaluated using AFM (Figure 10, A-B). Both nanoparticles showed a spherical shape and the average size of 2-20 nm. Furthermore, the Figure 10, B highlights the excellent dispersion of MNPs-2. TEM analysis for MNPs-2 was carried out to confirm the results obtained by AFM (Figure 10,C-D).
MNPs-1 and MNPs-2 were characterised by FT-IR (Figure 11). In the IR spectra, the broad peak around 3000-3500 cm^{-1} is due to the O-H stretching vibration and the peak at 1623 cm^{-1} can be attributed to the bending vibration of adsorbed water molecules. The presence of NH_4^+ on the nanoparticles surface can be confirmed by FT-IR spectroscopy. In the Figure 11, the MNPs-2 spectrum (red line) has a peak at 1427 cm^{-1} attributed to the deformation of NH_4^+ associated with a peak at 2979 cm^{-1} [142,143].

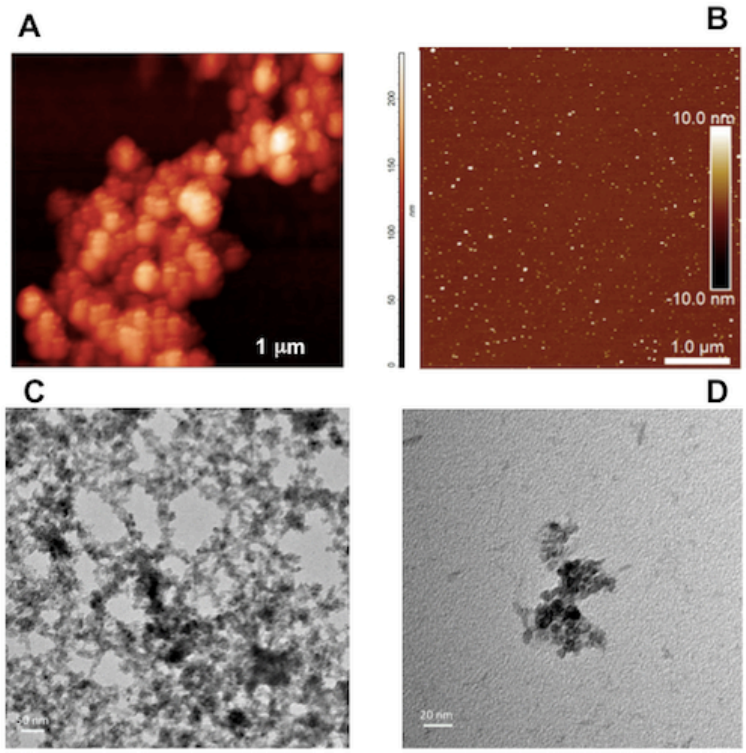

Figure 10 Characterisation of MNPs-1 and MNPs-2. A) AFM of MNPs-1; B) AFM of MNPs-2; C) TEM of MNPs-2 in 50 nm; D) TEM of MNPs-2 in 20 nm

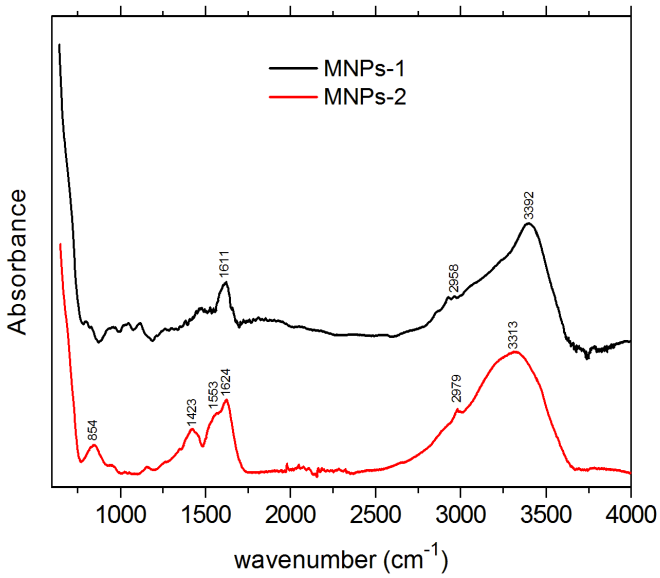

Figure 11 FT-IR comparison between MNPs-1 and MNPs-2

2.3 Laccase immobilisation on MNPs

Laccase from *Trametes versicolor* (*Tv*) was immobilised on magnetic nanoparticles following various procedures.

In MNPs-1 the laccase was immobilized through covalent bond. For this purpose the MNPs-1 were functionalized with amino groups using APTES. MNPs-1 (1 g, $4.32 \cdot 10^{-3}$ mol) were dissolved into EtOH (332 ml) [144]. Than, APTES (8.0 ml, 0.034 mol) was added to the Fe_3O_4 nanoparticles solution and its pH was adjusted to 5 by the drop-wise addition of HCl 1N (34.6 ml). After stirring at 25 °C for 24 h, the amino-coated Fe_3O_4 nanoparticles were collected using a permanent magnet, washed with ethanol three times and last time with ultrapure water, and then dried under nitrogen flux. The amino-coated Fe_3O_4 nanoparticles were dissolved into phosphate buffer (PBS) (100 Mm, pH 7.1) and sonication was performed on the solution for 15 min. Successively, to extend the spacer and facilitate the covalent attachment of laccase, the amino groups on the magnetic nanoparticles were linked to aldehyde groups by treating them with glutaraldehyde. The linker allows the higher mobility of the enzyme in the space, favouring the reaction with the substrate [66]. The glutaraldehyde solution was added to the solution, which was stirred at 150 rpm at 25 °C for 2 hours.
The sample of MNPs-1-APTES-glutaraldehyde were collected using the permanent magnet and washed with phosphate buffer three times to remove the unreacted glutaraldehyde [63]. The laccase solution was added to MNPs-1-APTES-glutaraldehyde complexes and the solutions stirred at 150 rpm at 25 °C for 16 hours.[145] Finally, the magnetic nanoparticles Fe_3O_4-Laccase were separated magnetically and washed two times with 0.5 ml of acetate buffer (100 Mm, pH 4.5) to remove the free enzyme. The washing buffer was collected for the determination of the activity. The activity of laccase immobilised on MNPs-1 was measured using the dye 3-Amino-4-hydroxybenzene sulfonic acid (0.25 mM) as a substrate in acetate buffer (pH 4.5). The formation of a coloured due to the oxidation of the substrate by the enzyme was analysed measuring the absorbance increase at 420 nm (ε/dm^3 mol^{-1} cm^{-1} 8600) with a UV-Vis Spectrophotometer [19].

Scheme 1. Schematic MNPs-1 immobilisation procedure

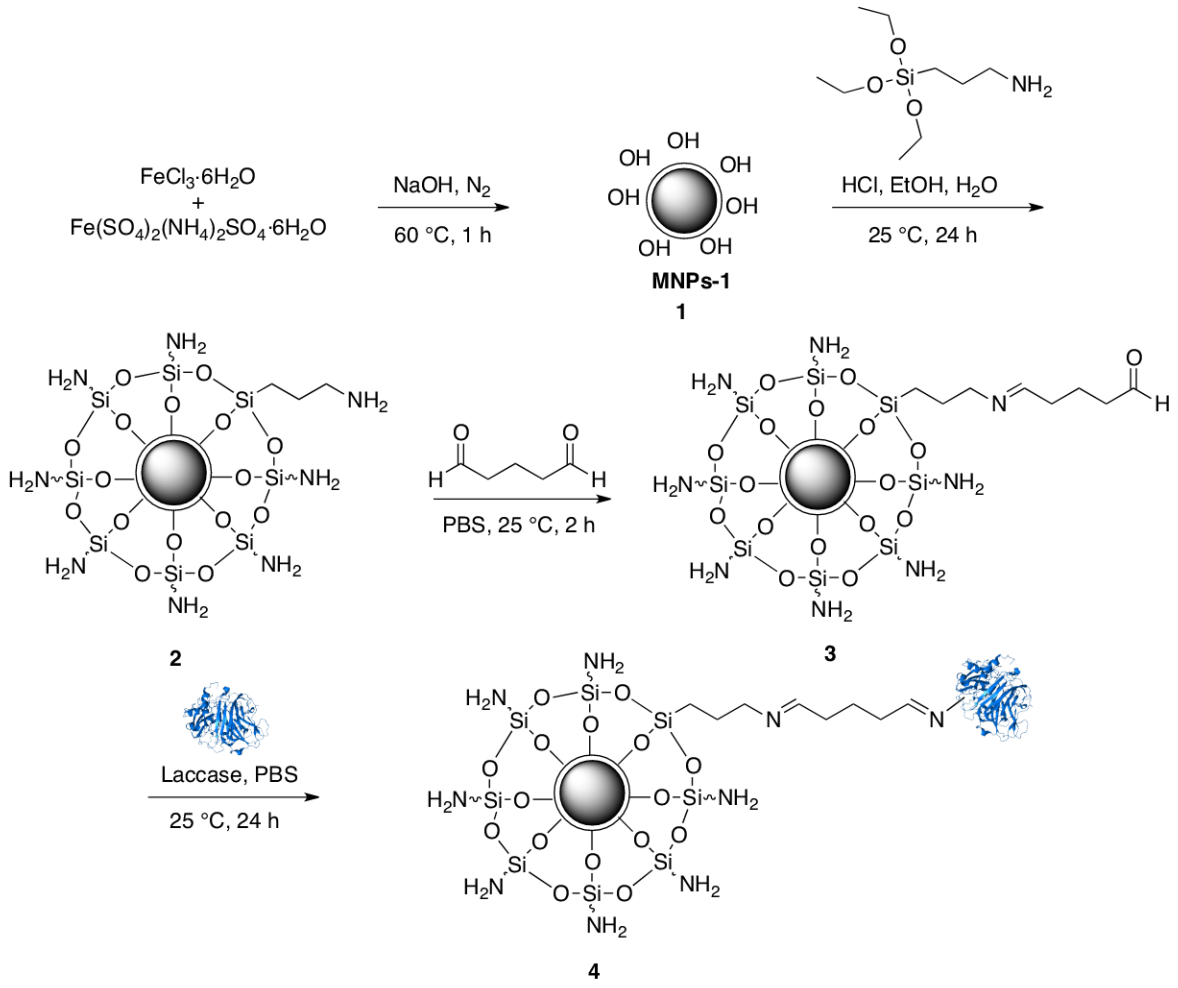

Laccase was immobilized on MNPs-2 using two different processes: the absorption and covalent binding. In the first case (Scheme 2, left side), the positivity of nanoparticles surface favours protein adsorption. Laccase were adsorbed on the nanoparticles surface because it has a net negative charge since its isoelectric point is around 3 [146,147]. The laccase solution was left to be absorbed directly to the nanoparticles and left to react at 25 °C in a shaker (150 rpm) for 16 hours. After that, the magnetic nanoparticles with laccase were separated from the solution using a magnet and washed one time with 1 ml of acetate buffer pH 4.5, 100 mM (**2A**, Scheme 2). The washing buffer was collected for the test activity.

In the second case (Scheme 2, right side), the presence of amino groups on the nanoparticles surface allows the binding with aldehyde groups of glutaraldehyde, and then, the enzyme bond.

Scheme 2. Schematic MNPs-2 immobilisation procedure

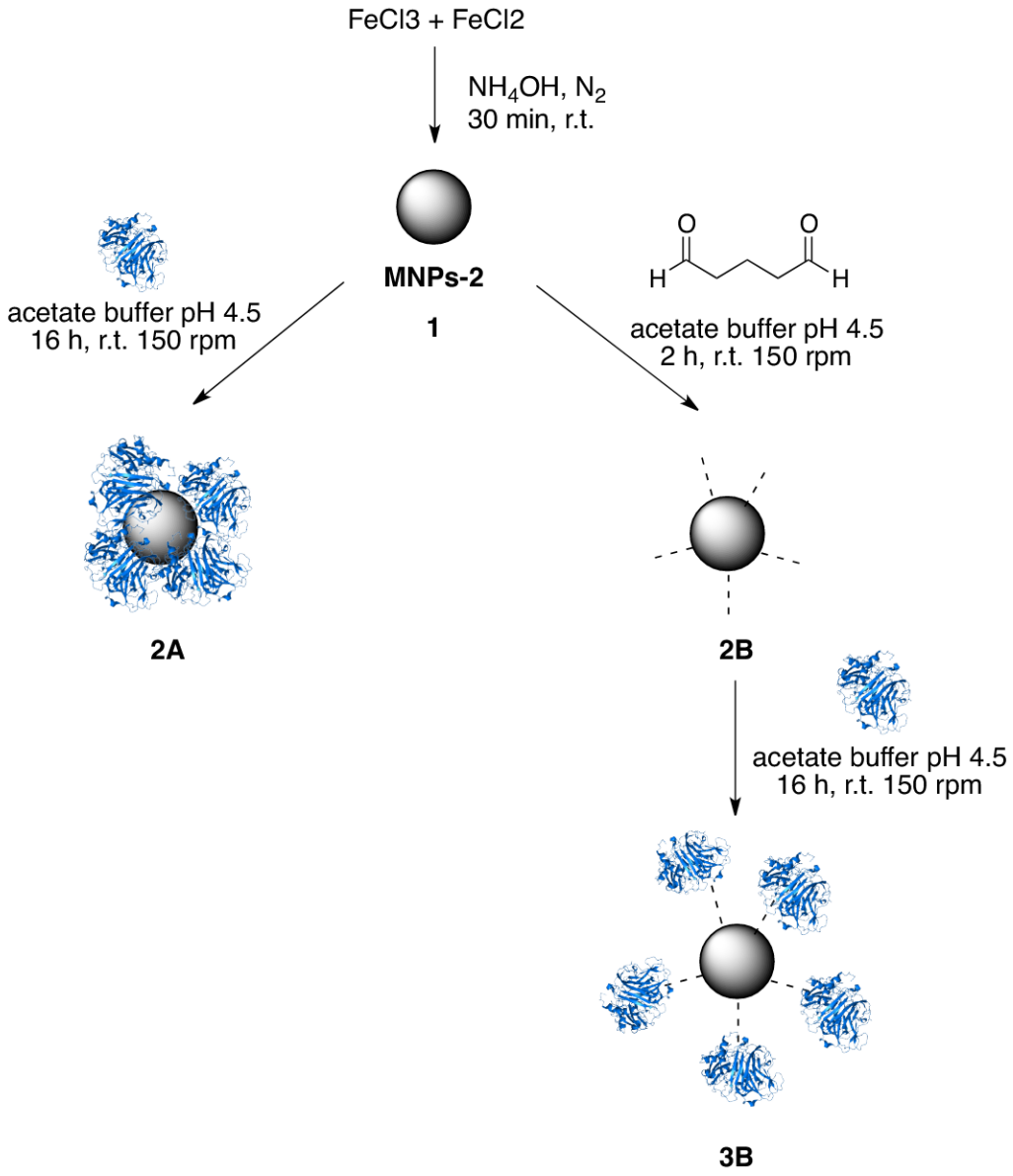

The magnetic nanoparticles were dissolved in 1 ml of acetate buffer (pH 4.5, 100 Mm) and the glutaraldehyde solution (0.5%) was added. The reaction was stirred at 150 rpm at 25 °C for 2 hours The sample was washed two times with 1 ml of acetate buffer using a magnet to

separate the solution from the nanoparticles (**2B**, Scheme 2). Then, the laccase solution was added and left to react for 16 hours at 150 rpm at 25 °C. Finally, the magnetic nanoparticles with linker and laccase were separated magnetically and washed one time with 1 ml of acetate buffer (**3B**, Scheme 2). The washing buffer was collected to analyze the activity. The activity of immobilised laccase for the other MNPs-2 route was measured using 2,2´-azino-bis (3-ethylbenthiazoline-6-sulphonic acid) (ABTS, 0.02 mM) as substrate in acetate buffer (pH 4.5, 100 mM), and the formation of product ($ABTS^{\cdot+}$) was analyzed measuring the absorbance increasing at 420 nm ($\varepsilon = 3.6 \times 10^4\ M^{-1}\ cm^{-1}$).

The enzymatic immobilization was confirmed by FTIR spectroscopy.
The FTIR spectra measured for the MNPs-1 functionalized with amino group (NH_2-MNPs 1), for the laccase conjugated to the NH_2-MNPs-1 (Laccase-MNPs-1) and for laccase are shown in Figure 12, A. The spectrum of the NH_2-MNPs-1 is similar to those reported in the literature for amino silanized magnetite NPs [148–151].
The intense band peaked at 990 cm^{-1} is due to the stretching of the Si-O-Si bonds of the silane coating [148,150]. The bands at ca. 1510 and 1615 cm^{-1} can be ascribed to NH_2 involved in hydrogen bonds and to free NH_2 groups, respectively.
The changes in the FTIR spectra after laccase immobilization on the NH_2-NPs are more clearly visible in the insect of Fig. 12,A, where the region from 1300 to 1800 cm^{-1} is shown. The peak at 1644 cm^{-1} in the middle curve corresponds to the amide I vibrational mode of the amide groups whereas the band at ca. 1530 cm^{-1} to the amide II vibrational mode. Probably, to the last band there is also a contribution from the unreacted amino groups at the surface of the NPs. In the Figure 12,B is possible to see the spectra of each product of the various immobilization steps on MNPs-2 with and without linker. The changes in the FTIR spectra after laccase immobilization were observed in the region 1250-1750 cm^{-1}.

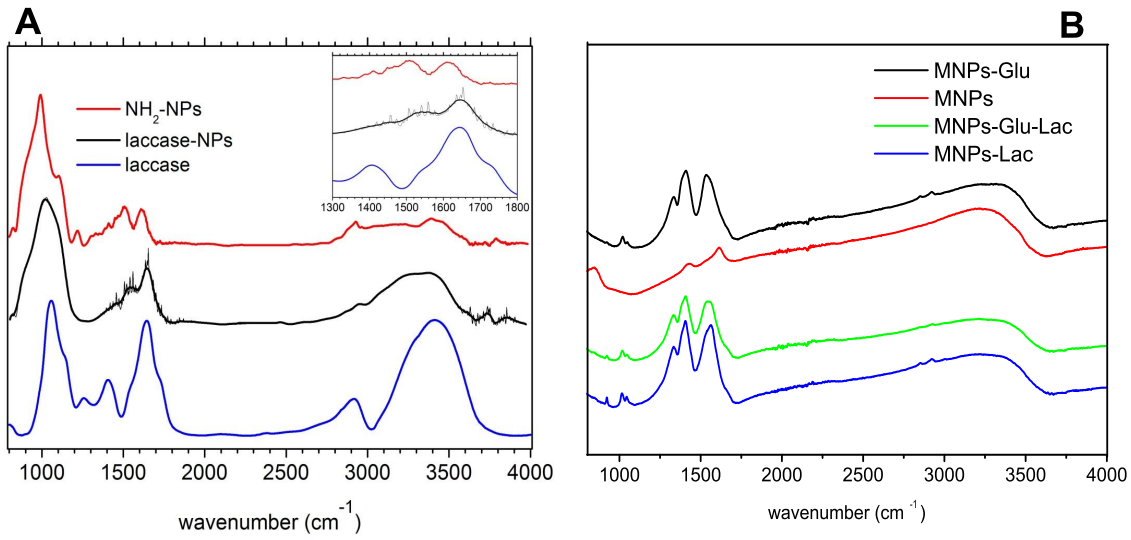

Figure 12: FT-IR characterisation for immobilisation process. A) FTIR spectra measured for the amino functionalized magnetite NPs (top curve), for the laccase immobilised on the amino functionalized NPs (middle curve) and for the pure laccase (bottom curve). In the top right of the figure the region between 1300-1800 cm^{-1} is shown. B) FTIR spectra for MNPs-2 with and without gluteraldehyde.

In order to optimize the immobilization conditions, various procedures were followed. The first approach was based on the change in the amount of support as shown in the first part of table 2. For MNPs-1, MNPs-2 with and without linker the same results were obtained showing that the best condition was 50 mg of support. Decreasing the weight of support the immobilization yield is reduced even if high activity was observed because almost all the immobilized laccase maintained activity. Instead, increasing the amount of support lower immobilization yield and activity are found. This probably happens because the aggregation of nanoparticles reduces the mobility of the enzyme and consequently it could be inactivated.

Using the same amount of nanoparticles (50 mg) different concentrations of Laccase (0.5, 1 and 2 mg/ml) were used to define the optimal conditions. The best results are obtained with 0.5 mg/ml of Laccase (Table 4).

All the experiments for MNPs-1 and MNPs-2 were carried out using 0.5% (v/v) of glutaraldehyde because the catalytic activity is inversely proportional to the percentage of linker used and extensive crosslinking may results in a distortion of enzyme structure and of the active site

conformation. Consequently the accessibility and accommodation of the substrate may be reduced [152].

Table 4 Optimization of immobilisation conditions testing different concentration of support, laccase and glutaraldehyde. All the experiments were carried out for three times.

	Support (mg)	**Immobilisation* yield (%)**	**Activity§ recovery (%)**
MNPs-1	25	35	94
	50	**78**	**65**
	100	57	15
MNPs-2 (with linker)	25	17	15
	50	**40**	**14**
	100	25	10
MNPs-2 (without linker)	25	23	18
	50	**47**	**30**
	100	30	30

	Laccase concentration	**Immobilisation* yield (%)**	**Activity§ recovery (%)**
MNPs-1	**0.5 mg/ml**	**87**	**50**
	1 mg/ml	80	43
	2 mg/ml	51	37
MNPs-2 (with linker)	**0.5 mg/ml**	**97**	**83**
	1 mg/ml	69	65
	2 mg/ml	60	53
MNPs-2 (without linker)	**0.5 mg/ml**	**87**	**75**
	1 mg/ml	54	46
	2 mg/ml	52	43

*Immobilisation yield (%)= immobilised activity/ starting activity x 100; §Activity recovery (%)= observed activity/ starting activity x 100

MNPs-1 and MNPs-2 with and without linker were reused for 10 cycles. For MNPs-1, laccase maintains the same activity for 10 consecutive reuses. Instead for MNPs-2 a small decrease of the activity was observed, but than it was stabilized (Figure 13).

According to these results, for the immobilization it seems more convenient to use MNPs-2 with 0.5 mg/ml of laccase solution (87% of

immobilization yield and 75% of activity), since it is easier to immobilize the enzyme in only one step. Moreover, it does not need the use glutaraldehyde that it is toxic.

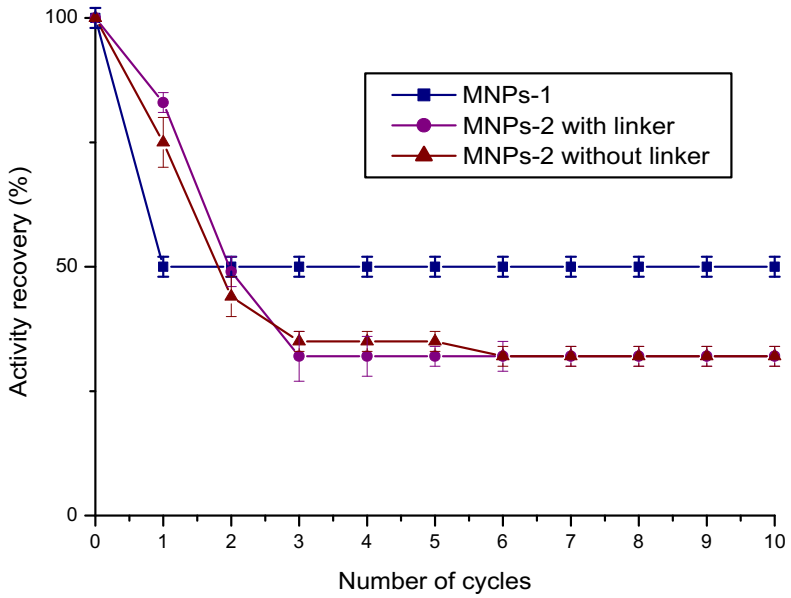

Figure 13: Reusability of laccase immobilised on MNPs-1, MNPs-2 with and without linker.

During the immobilization test a strange (an unexpected) behaviour was observed using ABTS as substrate. Usually, Laccase oxidises ABTS to form the stable cation radical $ABTS^{+}$ (Figure 14) [13].
The ABTS substrate is commonly used to test the laccase activity as the stable cationic radical formed originates a peak in the UV-vis spectrum at 420 nm which is used to follow the oxidation reaction. ABTS is added to the solution with immobilized laccase and then with magnet the solution is isolated from the MNPs with laccase. This solution is analysed by UV-vis spectrophotometry to determine by UV-visible analysis the enzyme activity.
The UV-vis analysis shows that the concentration of ABTS (responsible of the peak at 340 nm) decrease during the reaction with MNPs-1-laccase but the peak of the cation radical $ABTS^{+}$ at 420 nm is not observed (Fig. 15, A).

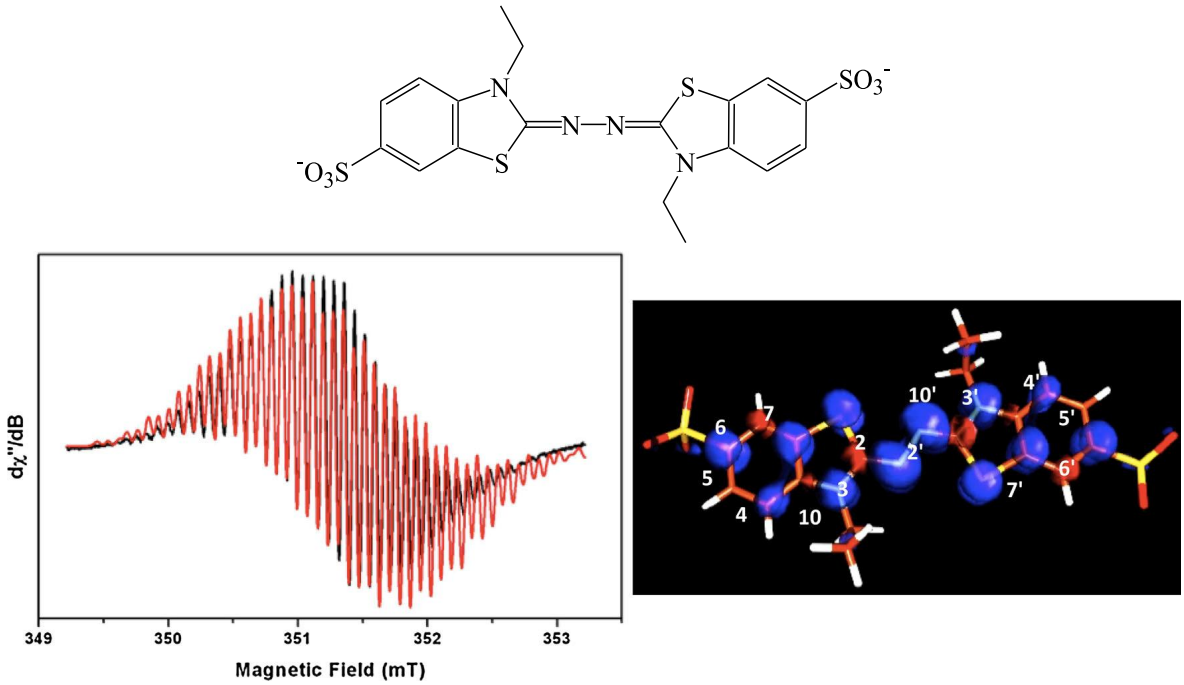

Figure 14: ABTS structure (Image above). Left. 298 K CW-EPR spectrum (X-band) of an ABTS solution formed upon oxidation by T. versicolor laccase (black trace) overlapped with its best simulation (red trace). The experimental parameters are as follows: 0.1 G modulation amplitude, 0.2 mW microwave power, and m = 9.86 GHz. The spectral parameters used for the simulation are given in Table 1. Right. B3LYP spin densities plot for the cation ABTS radical. The spin densities have been determined using a contour value of 0.003 with the program Molden. Blue positive spin densities; red negative spin densities [13].

The Fig. 15,B shows the results of the UV-Vis analysis of (normal) reaction between ABTS and free laccase monitoring using UV-visible.
To explain this (strange) behaviour it is hypothesized that the cation radical of ABTS was absorbed by the negatively charged MNPs-1. This hypothesis is supported by the FTIR spectra showing the presence of ABTS on the MNPs-1 surface after the reaction (Figure 16,A).

Instead, in the case MNPs-2 there is an electrostatic repulsion between the cation radical $ABTS^{+}$ and the MNPS-2 which are positively charged at pH=4.5 at which the reaction is carried out. Thus, it was possible to observe the absorption of the product in the solution and to test the immobilization activity using ABTS. These conclusions were also confirmed by FTIR analysis. The FTIR spectra of the MNPS-2 after

reaction with ABTS did not show the presence of the cation radical $ABTS^{+}$ (Figure 16,B-C).

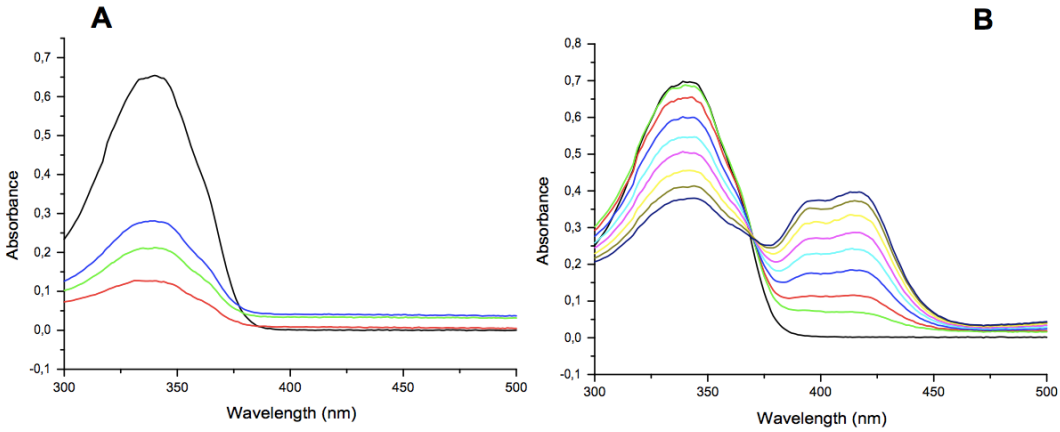

Figure 15: ABTS reaction. A) ABTS with laccase immobilised on MNPs-1 B) ABTS with free laccase

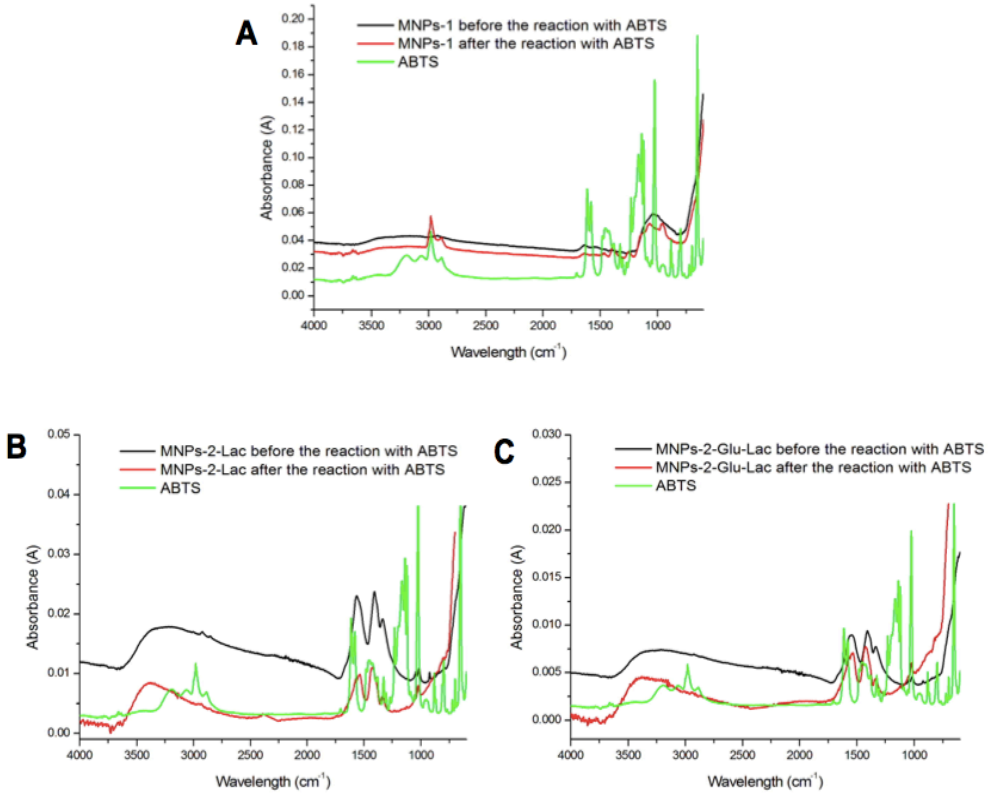

Figure 16: FT-IR of MNPs before and after the reaction with ABTS comparing with ABTS spectrum. A) MNPs-1 B) MNPs-2 without linker C) MNPs-2 with linker.

2.4 MNPs toxicity

When considering the usage of MNPs, toxicity is the major area of concern, as not much exploration has been done in this contest. The safety valuation of MNPs on cell lines (in vitro) is an easy, simple and inexpensive method as experiments can be controlled consistently [153]. MNPs toxicity has been linked to criteria like dose-dependency, time, surface modification, concentration, size, and shape parameters [154].

MNPs-1 in all steps of immobilisation were tested to investigate their toxicity. Percentage of viable NIH3T3 mouse fibroblasts after 24 and 48 hours of contact with different concentrations of test samples as determined by the Neutral Red Uptake (Figure 17).

Toxicity was higher as sample concentration increased, in fact from the literature the higher the number of nanoparticles, the higher risk they possess for toxic effects [155]. The contact time is another parameter that influences the toxicity. Figure 17 shows that nanoparticles increase their toxicity with increasing contact time, this effect was not observed for nanoparticles with immobilised laccase. In fact, the results obtained show the lower toxicity of nanoparticles with immobilised laccase than naked nanoparticles or nanoparticles coated with APTES and glutaraldehyde. The proven reduction of the toxicity of magnetic nanoparticles with immobilised laccase is an important advantage from the application point of view.

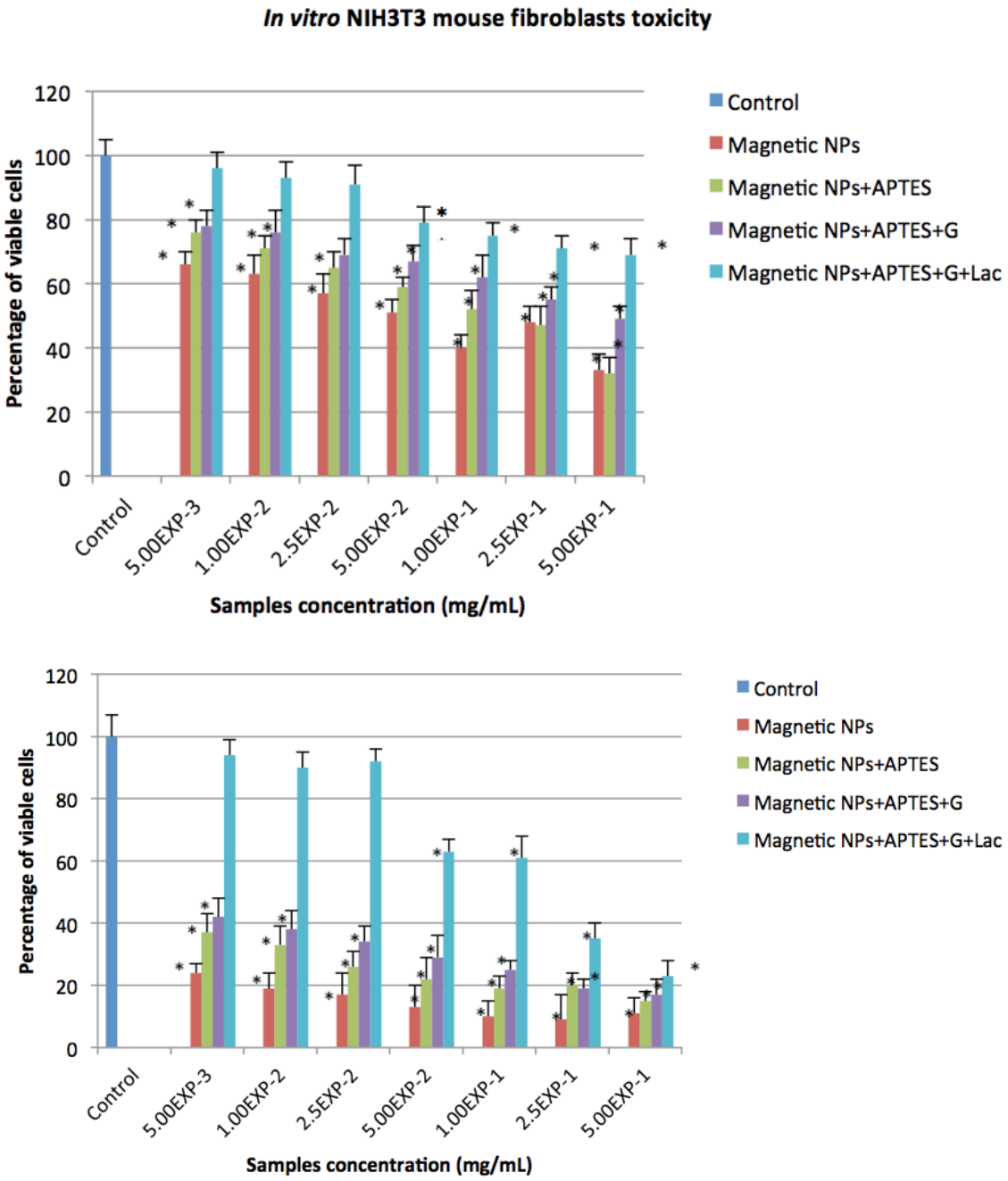

Figure 17: Percentage of viable NIH3T3 after 24 (image above) and 48 (image below) hours of contact with different concentration of test samples as determined by the Neutral Red Uptake. Data are mean ± SD of three experiments run in sic replicates. *Values are statistically different versus negative (complete medium), $p<0.05$.

2.5 Chitinase immobilisation on MNPs and CMS

This part of the chapter reports the immobilisation strategies for chitinase. The magnetic nanoparticles, previously described, together with chitosan beads, have been selected as supports for chitinase immobilisation.
For this study, an *exo*-chitinase named Chit42 was chosen and produced. The chitinase Chit42 from *Trichoderma harzianum* CECT2413 fused to the *Saccharomyces cerevisiae* MFα1 secretion signal was previously cloned in plasmid pIB4 and expressed in *Pichia pastoris* [34]. To express chitinase, *P. pastoris* strain was cultivated for about 24 hours in 500 mL of BMG-F composed by 13.4 mg/mL YNB, 4 mg/mL biotin, 1% (w/v) glycerol and 100 mM potassium phosphate, pH 6.0. Subsequently, the culture was grown in a 5 L bioreactor (Biostart BPluss Sartorius Ltd., Gottingen, Germany) containing 3.5 L of batch medium (40 g/L glycerol, 26.7 mL H_3PO_4 85%, 0.93 g/L $CaSO_4$, 18.2 g/L K_2SO_4, 14.9 g/L $MgSO_4$, 4.13 g/L KOH, 2 mL biotin (0.2 g/L), and 4.35 mL of PTM1 trace salts). The fermentation was carried out at 30 ºC, 600 rpm agitation, 20% dissolved oxygen and pH at 5 was controlled with NH_4OH 28% (v/v) for 24 hours (~40 OD600 units). To induce the expression of protein Chit42, methanol was added constantly during 4 days at 20 µL/min/L of fermentation volume (final ~290 OD600 units). Culture growth was monitored spectrophotometrically at 600 nm (OD_{600}) and protein concentration using NanoDrop at 280 nm. To obtain the pure protein from the expression medium, the cells were removed by centrifuging at 6000×*g* for 15 min, then the extracellular fraction was concentrated using 30000 MWCO PES membranes in a Vivaflow 50 system (Sartorius, Gottingen, Germany).

The activity of chitinase was analysed testing the reduction of sugars produced from colloidal chitin and chitosan [34].
Chitosan 1% (w/v) was prepared dissolving 1 g of chitosan in 100 mL of acetic acid (0.1 M) and the pH was adjusted to 5 with sodium acetate (1 M, pH 5.5). The enzymatic reactions were carried out adding 100 µL of the enzymatic solution, previously solubilized in potassium phosphate pH 5.5, 70 mM, to 400 µL of 1% (w/v) colloidal chitin and other

substrates. Than, the reactions were incubated at 35 °C and 900 rpm in a Termo Shaker TS-100 (Boeco, Hamburg, Germany) for 1 hour. Consequently, they were boiled for 10 min and one volume of 0.2 M NaOH was added. Finally, centrifugation at 12000×g for 5 min was used to remove the polysaccharides. The quantification of reducing sugars in the supernatant was carried out using 3,5-dinitrosalicylic acid (DNS) method adapted to a 96-well microplate scale and a calibration curve of D-glucosamine (0–3 mg/mL) was used [34]. The unit of chitinase activity (U) was defined as that corresponding to the release of 1 µmol of reducing sugar per minute (µmol/min).

Chit42 was immobilised on magnetic nanoparticles fallowing the traditional protocol described previously for MNPs-1, and on CMS.
Chitosan macro-spheres (CMS) were prepared applying the neutralization method. 2% (w/v) chitosan low molecular weight solubilized in 0.2 M acetic acid was agitated for 16 hours at room temperature. Than drop wise of viscous solution was coagulated in 0.5 M NaOH and 13% ethanol solution using a Cole Parmer™ Masterflex™ Brushless Pump System (Thermo Fisher Scientific). The formed chitosan beads were washed with water until neutral pH was reached [68,156]. To immobilised Chit42 on chitosan bead (CMS), glutaraldehyde (GA) and genipin (Gnp) were used like linker.

The size and morphology of magnetic nanoparticles (MNPs), before and after immobilisation of Chit42, were investigated using TEM (Transmission Electron Microscopy). The figure 18 (A) shows their spherical morphology and their average size of about 10 nm. After the immobilisation process (Figure 18 B), all complexes apparently showed the same size and shape to each other and to that previously obtained in literature [157,158].
The morphological characterisation of chitosan macro-spheres (CMS) was carried out using SEM (scanning electron microscopy) (Figure 18 C,D,E). CMS showed a size of 0.99 mm and their spherical form with bright and smooth surface was evident. It was observed that their size depend on the hydration, the wet and dry form was about 2 mm and 1

mm respectively, measured using millimetre paper, because they lost considerable amount of water [68].

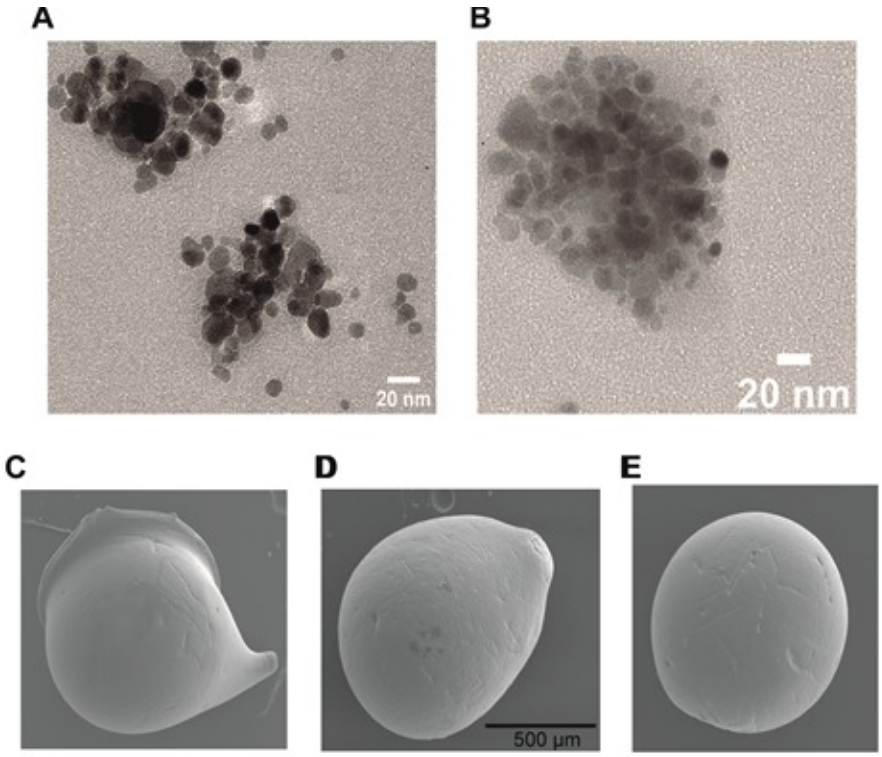

Figure 17 Characterisation of immobilisation systems using TEM for magnetic nanoparticles and SEM for chitosan beads. A) MNPs-GA; B) MNPs-GA-Chit42; C) CMS-GA; D) CMS-GA-Chit42 E) CMS-Gnp-Chit42. The same scale bars was used for C), D) and E).

In order to obtain an efficient immobilisation process, the conditions were tested and optimized.
The fist parameter was the amount of enzyme, different ratios of Chit42 per gram of support with 0,5 % (w/v) GA or 0.125% (w/v) were used.
The best results were reported in Table 5. For immobilisation of Chit42 on magnetic nanoparticles, 6,2 mg of Chit42 was the optimal amount, the immobilisation yield and the recovered chitinase activity were both of around 62-67%. Instead, by decreasing or increasing the concentration of the enzyme the recovery activity was less than 50%. For immobilisation on chitosan beads using GA or Gpn best results were obtained using 6.2 and 2 mg of protein/g of CMS beads, with a recovery activity of 71% and 62%, respectively and less than 40% and 60% of

recovery activity for CMS-GA and CMS-Gpn, respectively, when other conditions were used.

Table 5 Optimal ratios of enzyme per gram of support for immobilisation on magnetic nanoparticles (MNPs) and chitosan beads (CMS) using GA (0,5%) and Gnp (0,125%) like linker.

Support type	Chit42 (mg/g support)	Immobilisation yield (%)	Recovery of activity (%)
MNPs-GA	6.2	62.3	66.7
CMS-GA	6.2	57.0	71.0
CMS-Gnp	2	86.5	62.3

Furthermore, the effect of temperature and pH on the immobilisation chitinase activity was investigated (Figure 19). For chitinase immobilised on magnetic nanoparticles, the optimal catalytic temperature was at 35-40°C, similar to free Chit42. However, the enzyme immobilised was more thermostable because retained more than 60% of its activity after 1 h at 50 °C instead of about 20% retained by the non-immobilised enzyme (Figure 19 A,B).

The thermal stability was observed also for immobilisation on chitosan beads, which showed an optimal temperature of 45 ºC and retained 50% of its activity at 50ºC (Figure 19 C). This stabilization effect is well-reported in covalent immobilisation and it represents an important advantage for industrial applications [159]. Concerning the pH dependence, free enzyme showed optimal activity at pH 5.0-6.0 (Figure 19 A). However, the activity of the immobilised Chit42 increased remarkably at acidic pHs, and specially, when using chitosan beads and Gpn, which showed maxima activity at pH 4 and retained more than 80% of the activity at pH 3 (Figure 19 C). The formation of covalent bond through amino groups of the immobilised Chit42 can cause imbalanced partition of H^+ and OH^- concentrations resulting in the protein higher acidic stability. In addition, these covalent bonds could alter the conformational flexibility of Chit42 and alter the substrate binding process [44,160,161]. In any case, the higher acidic stability of the immobilised Chit42 gives this biocatalyst the advantage to act more

efficiently on chitin and chitosan, which are more soluble at acid pH values.

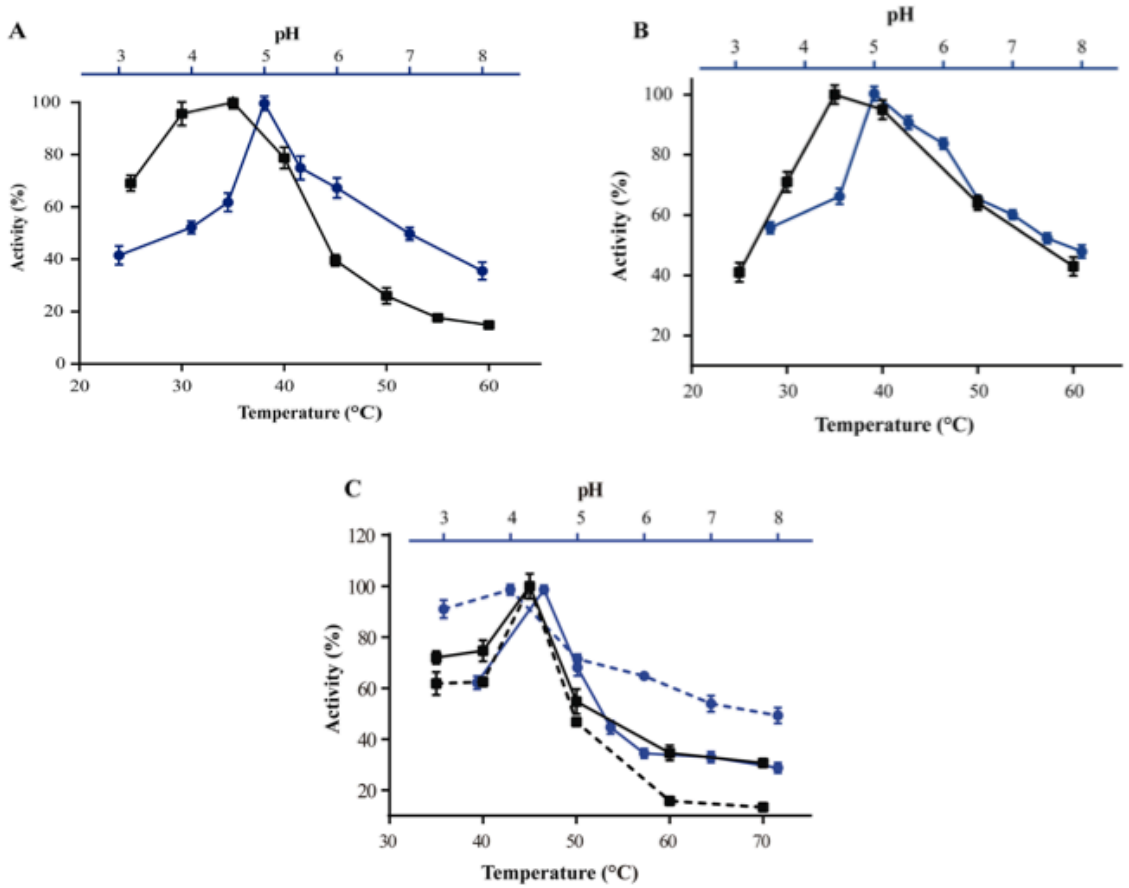

Figure 19 Effect of temperature and pH on the Chit42 free and immobilised. A) Temperature (black line) and pH (blue line) for free Chit42; B) Temperature (black line) and pH (blue line) for Chit42 immobilised on magnetic nanoparticles; C) Temperature (black continuous line) and pH (blue continuous line) for Chit42 immobilised on chitosan beads using GA and temperature (black discontinuous line) and pH (blue discontinuous line) for Chit42 immobilised on chitosan beads using Gpn.

The reusability of enzymes in industrial processes has a enormous economic relevance. In this context, the reuse of chitinase Chit42 immobilised on MNPS and CMS was investigated using batch reactions (Figure 20). After each cycle of reaction (1 h), catalysts MNPs-GA-Chit42 and CMS-GA/Gpn-Chit42 were separated from their reaction mixtures using external magnetic field and centrifugation, respectively. Before every one of the new reused cycles, all catalysts were washed in distilled water and phosphate buffer. The catalyst MNPs-GA-Chit42

retained higher than 70% of its initial chitinolytic activity after 2 cycles but only 30% after 5 cycles (Figure 20 A). Regardless of the linker used in the enzyme immobilisation on chitosan beads, these biocatalysts were more negatively affected after washes. The catalyst CMS-GA-Chit42 completely lost its activity after the second cycle, whereas CMS-Gnp-Chit42 retaining about 30% (Figure 20 B). In addition, the loss of activity during recovery steps due to possible outflow of the enzyme from the support was also investigated, but no free enzyme was detected on the washing buffer. Loss of chitinase activity after immobilisation on MNPs and CMS have previously reported using commercial chitinases, which retained less of 20% of their initial activity after only 2 reuse cycles [84,162].

To try to stabilize bonds between enzymes and supports, the reduction with sodium borohydride, which converts weak Shiff's bases into stable secondary amino bonds was previously used [156]. The influence of this reducing agent on the immobilised Chit42-catalysts was also evaluated (Figure 20). The reduction of the immobilised catalyst caused a clear decrease of the initial Chit42 hydrolytic activity, of about 50% (from 1.0 to 0.52 units), 70% (from 1.5 to 0.42 U) and 33% (from 1.3 to 0.86 U) in the catalysts MNPs-GA-Chit42, CMS-GA-Chit42 and CMS-Gpn-Chit42, respectively. However, the reduction clearly improved the reusability of the immobilised Chit42, the MNPs-GA-Chit42 catalyst being the most favoured and retaining more than 50% of its activity after at least 5 cycles of reuse (Figure 20).

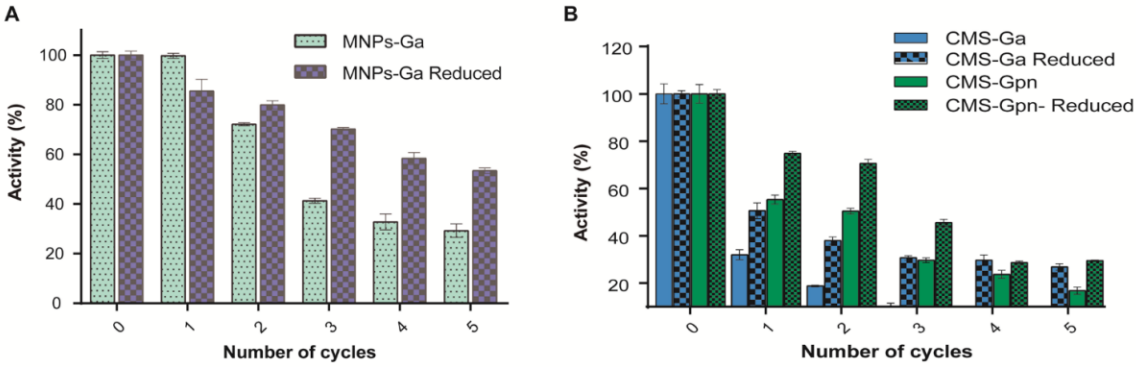

Figure 20 Reusability of Chit42 immobilised on (A) MNPs and (B) CMS. Assays were conducted in triplicate and data are means of three parallel measurements. Standard errors are indicated.

2.6 COS production and characterisation

The hydrolytic activity of the free Chit42 and immobilised Chit42 was investigated using different chitinolytic materials (Table 6). Both free and immobilised chitinase showed maximum hydrolytic activity on colloidal chitin and with more activity on small chitosan with DD 77-81 than in larger ones with DD >90. In addition, immobilised enzyme had at least 3 times higher hydrolytic activity than free enzyme on any of the chitosan tested. Curiously, Chit42 immobilised on chitosan beads-GA hydrolyzed commercial chitosan CHITS and colloidal chitin with the same effectiveness.

Table 6 Hydrolytic activity of free and immobilised Chit42 using different substrates. Data are means of three independent experiments and standard errors are indicated.

			Hydrolitic activity of Chit42 (%)			
Substrate	**MW (kDa)**	**DD (%)**	**Free**	**MNPs-GA**	**CMS-GA**	**CMS-Gnp**
Colloidal Chitin	n.d.	≤8	100.0 ±2.9	100.0 ±4.2	100.0 ±2.4	100.0 ±8.2
QS1	98	81	14.8 ±3.5	46.5 ±6.1	69.0 ±1.6	44.9 ±4.0
QS2	31	77	13.5 ±0.8	50.8 ±8.0	60.7 ±5.3	49.2 ±4.0
CHIT100	100-300	>90	9.8 ±3.5	34.2 ±1.9	43.8 ±1.4	34.5 ±7.2
CHIT600	600-800	>90	4.2 ±3.6	3.1 ±2.8	14.6 ±1.9	16.3 ±4.5
CHIT50	50-190	77	16.0 ±0.8	72.2 ±4.2	98.0 ±3.0	43.5 ±8.6

The production of COS using immobilised Chiti42 was characterised using HPAEC-PAD chromatography and mass spectrometry analyses [163].

Figure 21 A showed that chitobiose ($(GlcNAc)_2$) was the main product obtained from colloidal chitin, followed by $(GlcNAc)_3$ and GlcNAc when using the immobilised enzyme. In addition, a large number of masses corresponding to different series of fully acetylated (faCOS) and partially acetylated COS (paCOS) were detected using mass spectrometry analyses (Figure 20 B, C, D). Specifically, masses corresponding to faCOS of $(GlcNAc)_{1-9}$ units and the paCOS GlcN-$(GlcNAc)_{1-3,5-7}$, $(GlcN)_2$-$(GlcNAc)_{1-3}$, $(GlcN)_3$-$(GlcNAc)_{2,4}$, $(GlcN)_4$-$(GlcNAc)_5$ were

detected (Figure 21). As expected, masses corresponding to $(GlcNAc)_2$ followed by $(GlcNAc)_3$ being the majority. Concerning paCOS, masses corresponding to GlcN-$(GlcNAc)_2$ followed of GlcN-$(GlcNAc)_3$ were the majority detected when using MNPs but that of GlcN-GlcNAc followed by GlcN-$(GlcNAc)_2$ when using CMS. Pattern of products obtained could have been slightly altered due to the support used, which could alter the structure/specificity of the protein. Especially, considering that when free Chit42 was previously used in the hydrolysis of colloidal chitin only masses corresponding to the faCOS of $(GlcNAc)_{1\text{-}4}$ units and the paCOS GlcN-$(GlcNAc)_{2,4}$ and $(GlcN)_2$-$(GlcNAc)_3$ were detected. However, despite the high number of compounds detected in mass spectrometric analyses, only the faCOS of $(GlcNAc)_{1\text{-}3}$ units could be clearly identified due to the availability of the corresponding commercial standards.

The Chit42 immobilised showed a higher range of product variability from colloidal chitin than the free enzyme. In fact, immobilisation can affect the adsorption of the substrate on the enzyme active site, confronting the catalytic residues and thus modifying enzymatic activity, selectivity and final product profile [164,165].

Analysis of the reaction products obtained when using immobilised Chit42 was performed on chitosan QS2 since it was the smallest one with the highest degree of acetylation, among those used. All HPAEC-PAD chromatographic profiles were very similar to each other, and with numerous signals (Figure 22). Both HPAEC-PAD and mass spectrometry analysis again confirming $(GlcNAc)_2$ as the main product (Figure 22, peaks (2)), but no mass of $(GlcNAc)_3$ was detected likely because chitosan was only poorly acetylated (DD of 77%). In addition, masses corresponding to the paCOS $(GlcN)_{1\text{-}3,5}$-$(GlcNAc)_{2\text{-}3}$ and $(GlcN)_{1–8}$-GlcNAc (represented on the right of Figure 21) were also detected. Again, same majority masses of paCOS were not obtained when using MNPs or CMS. Thus, masses of GlcN-$(GlcNAc)_2$ and GlcN-GlcNAc continued to be the majority when using MNPs and CMS, but this time followed by that of GlcN-GlcNAc and $(GlcN)_2$-GlcNAc, respectively. Mass of $(GlcN)_2$-GlcNAc was that of the majority COS (faCOS or paCOS) previously produced by the free enzyme on chitosan, which allowed to suggest that the highest peak obtained by

HPAEC-PAD could also be due to this trisaccharide [163]. Therefore, the highest peak produced by the free Chit42 (Figure 22, in profile I, to the right of GlcN, (1) signal) would also correspond to $(GlcN)_2$-GlcNAc as explained in the previous study. In order to analyze this product discrepancy, masses of COS obtained by hydrolysis of chitosan CHIT600 were also analyzed. However, as it has happened before with the free enzyme, the most abundant mass of the reaction corresponded to $(GlcN)_2$-GlcNAc regardless of the type of support used in the immobilisation.

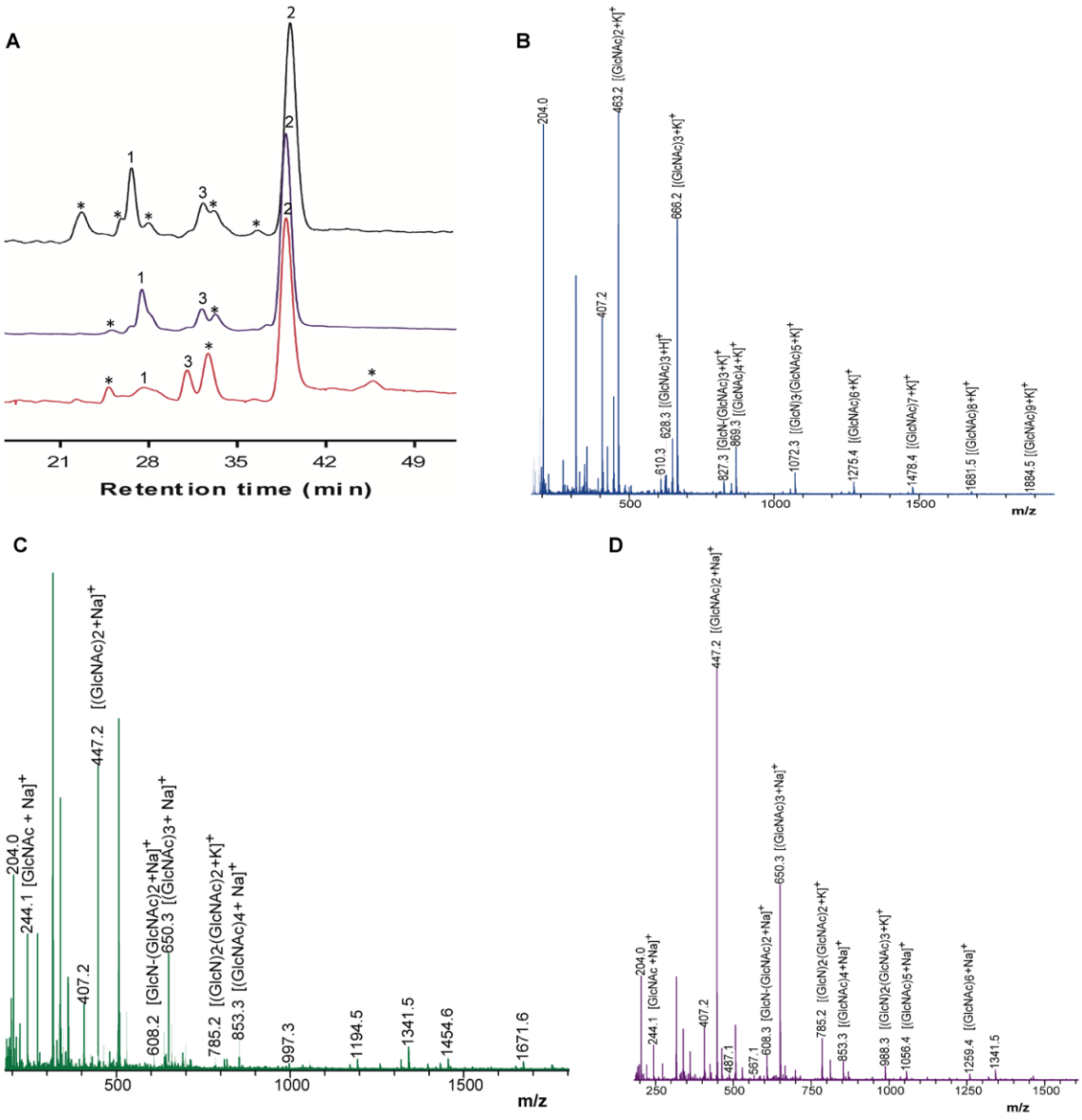

Figure 21 Analysis of COS obtained from colloidal chitin. (A) High-performance anion exchange chromatography (HPAEC-PAD) analyses. The

24 h reactions catalyzed by immobilised Chit42 on MNPs (red) and CMS using GA linker (blue) and Gpn (black). Peaks: (1) GlcNAc; (2) $(GlcNAc)_2$; (3) $(GlcNAc)_3$; (*) Unidentified. MALDI-TOF MS analysis of the COS mixtures formed with the enzyme immobilised on (B) MNPs-GA, (C) CMS-GA and (D) CMS-Gpn. The peaks in the spectra correspond to the monoisotopic masses of hydrogen adducts $[M+H]^+$, $[M+K]^+$ and $[Ma+Na]^+$ of the COS. Only the major identified products were marked.

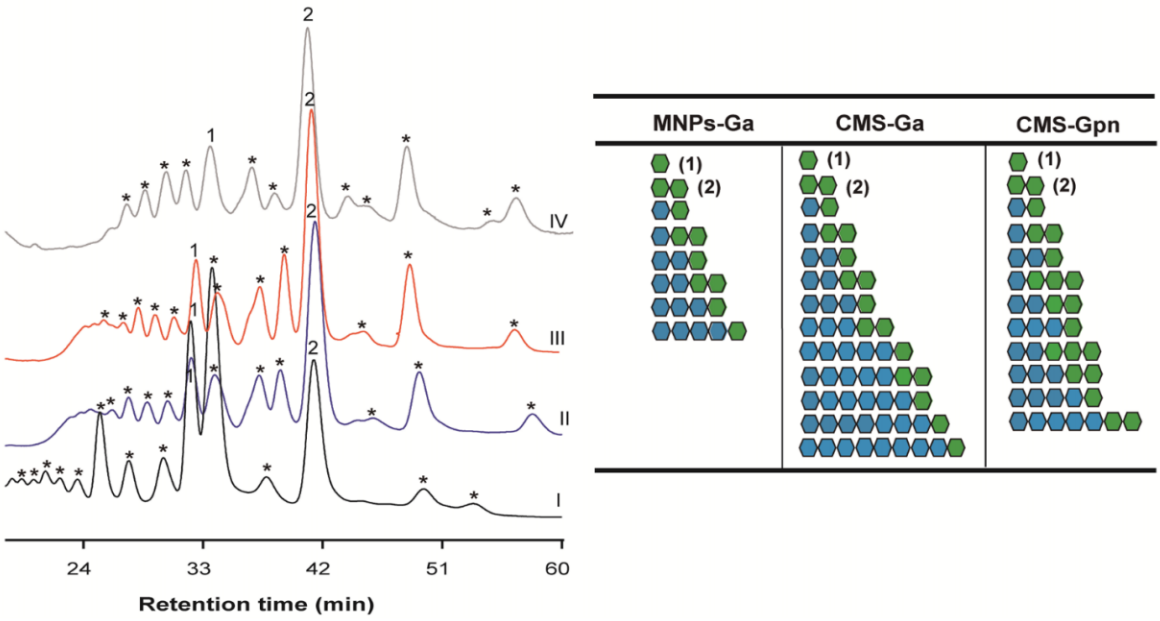

Figure 22 HPAEC-PAD analysis of COS produced by the immobilised Chit42 with chitosan QS2 as substrate. On the right, a schematic representation of the polymerization degree and composition of reaction products predicted from mass spectrometry data is presented. Blue circles: GlcN. Green circles: GlcNAc. Identified peaks: (1) GlcNAc; (2) $(GlcNAc)_2$. Chromatograms obtained with I: free enzyme; II: MNPs-GA-Chit42; III: CMS-GA-Chit42; IV: CMS-Gpn-Chit42.

Structure of Chit42 was previously determined, and showed the expected folding described for chitinases included in the family GH18 with a characteristic groove shaped substrate-binding size able to accommodate at least six sugars units [163]. The unusual substrate-assisted catalytic mechanism of chitinases-GH18 requires a glutamic residue in the protein chain providing the acid protonating the glycosidic bond to be hydrolyzed and a mandatory GlcNAc residue in the substrate (after which to cut), which provides the oxygen (of the N-acetyl group)

acting as nucleophile. Therefore, to a greater acetylation degree of substrate, greater hydrolysis and higher diversity of products formed as previous reported,[34,166], which led us to use the smallest substrate with the highest degree of acetylation (chitosan QS2) in this section.

To our knowledge no paCOS produced by immobilised chitinases has been previously reported. It is conceivable that the use of supported enzymes (1 h contact time with substrate in a thermo shaker before products analysis) reduces substrate crystallinity making the crystalline regions more accessible to the hydrolytic enzyme activity with high yield of low molecular weight products (see Table 6). This represents an interesting achievement, for the industrial bioconversion of chitinolytic polymers, as with the use of supported enzymes the pretreatment of substrate might be avoided. A deeper understanding on how the immobilised enzyme produces paCOS and the structural aspects involved in this process will be essential to improve the enzyme activity/specificity to produce COS with different characteristics and, a priori, properties.

PRODUCTION AND CHARACTERISATION OF BIOMATERIALS

In this chapter, the enzymatic production and characterisation of biomaterials as have been reported. Particularly, it is focused on the enzymatic synthesis and analysis of insoluble and soluble melanin pigments.

Laccase from *Trametes versicolor* (*Tv*) was used to produce melanin pigments from 3,4-dihydroxyphenylalanine (dopa), in presence or absence of cysteine. These laccase-derived melanins were used as references for spectroscopical features of dopa-melanin (eumelanin) and cysteinyldopa-melanin (pheomelanin).

The pigments were used to investigate the composition of paramagnetic pigment produced by the bacteria *Streptomyces cyaneofuscatus* (Sc-Ms1) and by the oxidative action of its derived tyrosinase, on dopa. The water-soluble pigment produced by the bacteria was identified as a mixture of dopa-melanin and for the most part of cysteinyldopa-melanin. The pigment produced by the bacterial tyrosinase instead was identified as a mixture of dopa-melanin with presence of cysteinyldopa-melanin traces.

The samples were characterised using S, X and Q-band CW multifrequency EPR. Furthermore, the pigments were also differentiated according to their relaxation properties using Q and X-band CW power saturations acquisitions and Q-band picket fance saturation recovery (PFSR) experiments.

Pulse EPR was proven a successful tool for the differentiation of melanin samples according to their relaxation rates, confirming the qualitative trend obtained with CW power saturation experiments.

Melanins exhibit important physic-chemical properties and in recent years they have been proposed for several biotechnological applications in optoelectronics, biomaterials functionalization and biomedical sectors. However, its insolubility represents a limit for some applications. In this context, laccase was used to synthetize soluble pyomelanins from Homogentisic Acid (HGA) and Gentisic Acid (GA). The spectroscopic characterisation and antioxidant activity determination were carried out for these soluble pigments.

3.1 Pigments production

Dopa-melanin (eumelanin) was synthetized using *Tv* laccase (12.9 U mg^{-1}) in 100 mM phosphate buffer at pH=7 in the presence of an excess of dopa (6.57 mg/mL) as substrate (1:1000 Lac:dopa molar ratio) [167]. The reactions were followed for 16 hours. The formation of an insoluble black pigment was obtained.
Cysteinyldopa (pheomelanin) was synthesized using *Tv* laccase (12.9 U mg^{-1}) with a dopa:cysteine 1:2 molar ratio in phosphate buffer pH=7 and in acetate buffer 100 mM (pH=4.5). A reddish powder was obtained [167]. Samples were dried under nitrogen flux for approximately 5 hours and then analyzed in the powder form.
A strain belonging to the *Streptomyces cyaneofuscatus* Pridham et al. 1958 species, referred to as "Sc-Ms1", was isolated from Algerian Sahara soil. It was investigated for its ability to produce melanin by the activity of an extracellular tyrosinase; this enzyme was then isolated and characterised [168].
Sc-Ms1 tyrosinase was produced by growing the strain in MPPM broth (glycerol 10 g/L, glucose 10 g/L, soya flour 10 g/L, casamino acids 5 g/L, yeast extract 5 g/L, 4.0 CaCO3 4 g/L, bacteriological agar 15 g/L, 1 ml of trace salts solution [g/100 ml: 1.0 FeSO4, 0.9 ZnSO4, 0.2 MnSO4], pH 7.0) supplemented with 1 mM filter sterilized $CuSO_4$ for 72 hours. After the centrifugation of bacterial cells presents in the medium, the tyrosinase enzyme was purified [168]. Ammonium sulphate 65% was used to precipitate the proteins, followed by the resuspension in potassium phosphate buffer (pH 6.5, 50 mM). The solution was dialyzed at 4°C for 24 hours against the same buffer and than it was concentrated by replacing the dialysis buffer with a 20% (w/v) polyethylene glycol 8000 solution (in 50 mM potassium phosphate buffer, pH 6.5) and incubating at 4°C for 24 hours. The concentrated solution was finally dissolved in 50 mM potassium phosphate buffer and applied to a DEAE Sephadex TM A-50 using batch technique to separate the enzyme from melanin.
Melanin was purified from the culture broth of Sc-Ms1 by precipitation in acidic environment. HCl 6 N was added to the solution until melanin

precipitation. Next, the precipitate was separated from the solution by centrifugation at 10.000 rpm for 10 minutes at 4 °C, and it was rinsed with deionized water until the pH became neutral.
Tyrosinase activity was tested with different mono- di- and tri- phenols [168]. The Sc-Ms1 tyrosinase showed a higher specificity for diphenols than monophenols. The low monophenolase/diphenolase activity is a common feature shared with other plant and bacterial tyrosinases [169–171]. Sc-Ms1 tyrosinase (47.6 U mg^{-1}) derived from the bacterial strain was employed to produce melanin in the presence of excess dopa (6.57 mg/mL) in phosphate buffer (100 mM, pH 7).

3.2 UV-Vis and FT-IR characterisation of melanin pigments from bacterial and enzymatic synthesis

The investigation of melanin structure represents an important point for their applications. Melanin pigments are known to exhibit a characteristic trend in their UV-Vis spectra. The samples displayed a monotone increase of radiation absorption toward lower wavelengths [172]. In Figure 23 the spectra of the bacterial melanin (red line), dopa-melanin tirosynase (black line) and dopa- and cysteinyldopa laccase (blue and green lines respectively) were compared. Their absorption profiles don't present detectable differences. The monotonic increase absorbance for the poorly solubilized eumelanin was associated to scattering effects which are less effective in soluble natural melanins [172]. Anyway, the correlation between the absorption spectrum of melanin with their chemical structure has been the object of several studies. A model based on an interplay of geometrical order and disorder of eumelanin aggregate structures has been successfully used to describe the absorption spectra by a first-principles computational investigation [173].
In Figure 24 are reported the FT-IR spectra of the samples. A broad absorption band in the region of 3400 cm^{-1} due to the stretching vibrations of -OH and $-NH_2$ groups, is presents in all spectra. Features centered around 2900 cm^{-1} are present in all melanin samples and can be attributed to the vibrations of CH_2 groups. The band at 1600 cm^{-1} is due to the C=O stretching vibration mode. The presence of the C-S

stretching vibration peak at 700-600 cm^{-1} is usually used to identify the presence of pheomelanin in natural samples [174,175]. This peak is evident in the cysteinyldopa sample (Figure 24c) and is present with less intensity in the bacterial sample (Figure 24a) confirming the presence of pheomelanin. Furthermore the IR profiles of these spectra are very similar. At the same time the IR spectrum reported in Figure 24b (Sc-Ms1 tyrosinase dopa melanin) is very similar to that reported in Figure 24d (*Tv* laccase dopa-melanin) with traces of the presence of the peak around 600 cm^{-1}.

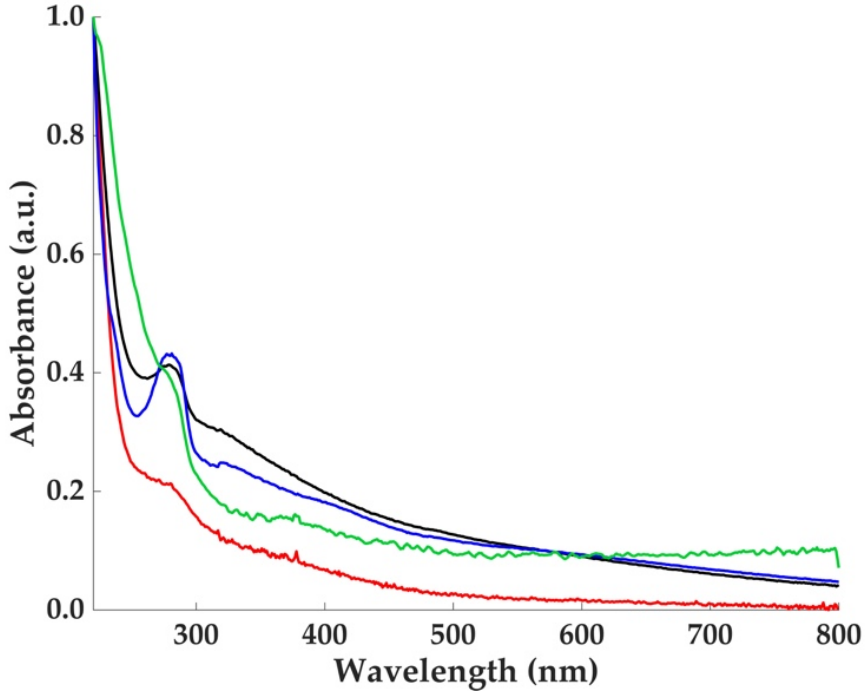

Figure 23 UV-Vis spectra of Sc-Ms1 melanin (red line), melanin pigment synthesized by Sc-Ms1 tyrosinase (black line), dopa (blue line) and cysteinyldopa (red line) melanin pigments synthesized by *Tv* laccase.

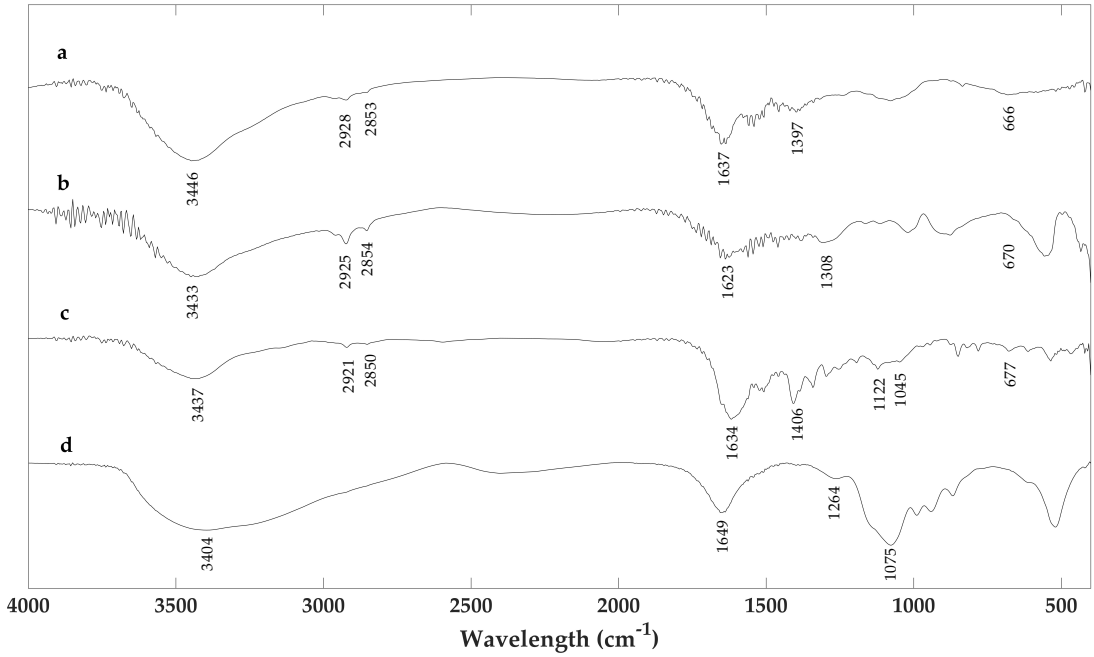

Figure 24 FT-IR spectra of (a) Sc-Ms1 melanin, (b) Sc-Ms1 tyrosinase dopa-melanin, (c) *Tv* laccase cysteinyldopa melanin, (d) *Tv* laccase dopa-melanin, respectively. All the spectra are recorded in transmittance mode.

3.3 S-, X- and Q-band Multifrequency EPR analysis of melanin pigments

UV-Vis and FT-IR are usually used for the investigation of pigments, but the EPR spectroscopy is the unique technique that can give more information about the structure and the identification of melanin types. In fact, it allows the study of free radical signals contained in the pigments. Melanin pigments are characterised by a persistent EPR signal due to the presence of exceptionally stable free radical [167,176,177].
Melanins are commonly studied at X-band frequencies (≈ 9 GHz), where a persistent asymmetric free radical signal with g-factor ≅ 2.0032 for pure eumelanin and 2.0050-2.0055 for pure pheomelanin, is detected [126,178]. A multifrequency EPR analysis allows to obtain more detailed information. The use of lower frequencies (e.g. 4 GHz) is necessary to generate a more symmetric signal for precise g isotropic value determination, while higher frequencies (e.g. 34 GHz) are required to resolve any complex spectra feature which would otherwise be hidden in absence of stronger magnetic fields [179,180]. This approach was